



Cite this: *Lab Chip*, 2025, **25**, 806

Bone microphysiological models for biomedical research

Francisco Verdugo-Avello, ^{*a} Jacek K. Wychowaniec, ^b
 Carlos A. Villacis-Aguirre, ^a Matteo D'Este ^b and Jorge R. Toledo ^a

Bone related disorders are highly prevalent, and many of these pathologies still do not have curative and definitive treatment methods. This is due to a complex interplay of multiple factors, such as the crosstalk between different tissues and cellular components, all of which are affected by microenvironmental factors. Moreover, these bone pathologies are specific, and current treatment results vary from patient to patient owing to their intrinsic biological variability. Current approaches in drug development to deliver new drug candidates against common bone disorders, such as standard two-dimensional (2D) cell culture and animal-based studies, are now being replaced by more relevant diseases modelling, such as three-dimension (3D) cell culture and primary cells under human-focused microphysiological systems (MPS) that can resemble human physiology by mimicking 3D tissue organization and cell microenvironmental cues. In this review, various technological advancements for *in vitro* bone modeling are discussed, highlighting the progress in biomaterials used as extracellular matrices, stem cell biology, and primary cell culture techniques. With emphasis on examples of modeling healthy and disease-associated bone tissues, this tutorial review aims to survey current approaches of up-to-date bone-on-chips through MPS technology, with special emphasis on the scaffold and chip capabilities for mimicking the bone extracellular matrix as this is the key environment generated for cell crosstalk and interaction. The relevant bone models are studied with critical analysis of the methods employed, aiming to serve as a tool for designing new and translational approaches. Additionally, the features reported in these state-of-the-art studies will be useful for modeling bone pathophysiology, guiding future improvements in personalized bone models that can accelerate drug discovery and clinical translation.

Received 12th September 2024,
 Accepted 24th December 2024

DOI: 10.1039/d4lc00762j

rsc.li/loc

1. Introduction

Bone disorders are prevalent worldwide, and a vast majority of them still lack an ideal therapeutic treatment. Frequently, the elderly population experiences considerable pain and some degree of disability, whereas many younger people are often affected by injury-related bone disorders. A recent report estimated that 1.71 billion people have a musculoskeletal condition in the world, such as bone cancer and osteoporosis, among many others.¹ For example, osteoporosis alone is affecting more than 200 million people, causing some degree of disability and predisposition to fractures, overall contributing to the global need for rehabilitation. Moreover, due the permanent crosstalk of bone with different cells, tissues, and organs, inevitably the presence of bone-related conditions may increase the clinical



Francisco Verdugo-Avello

Francisco Verdugo-Avello is a dental surgeon (DDS). He obtained his MRes in Tissue Engineering at the University of Manchester, United Kingdom and currently is a PhD candidate in Molecular Biotechnology from Universidad de Concepción, Chile. He is currently working in tissue engineered modelling of bone cancer and preclinical development of organoid-based *in vitro* diagnostics, bone bioprinting and

*microphysiological systems for cancer research. His interests are development of new *in vitro* diagnostics for bone metastasis and hydrogels for bone biofabrication. His expertise lies in multidisciplinary biomedical project research and development by gathering *in vitro* data alongside clinical processes.*

^a Biotechnology and Biopharmaceuticals Laboratory, Departamento de Fisiopatología, Facultad de Ciencias Biológicas, Universidad de Concepción, Víctor Lamas 1290, P.O. Box 160-C, Concepción, Chile. E-mail: frverdugo@udec.cl; Tel: +56 9 79367712

^b AO Research Institute Davos, Clavadelstrasse 8, 7270, Davos, Switzerland



risk of developing associated cardiovascular and/or mental diseases.² Most of these bone disorders are still treated with suboptimal therapies, and many only have dietary supplement indications or endless treatment ladders (e.g. by anti-inflammatory drugs) that do not effectively target the root cause of the disease, but merely its symptoms.³

Bone tumours and metastases are major sources of human suffering, for which treatments are still suboptimal. One cause of insufficient therapeutic efficacy is the interpersonal biological variability, which is in stark contrast with the therapeutic design focused on a standard or average patient.⁴ Nowadays, it is known that bone homeostasis

maintained by the cellular component is altered by the interactions produced by cancer cells, which is usually evidenced by an overexpression of cytokines that stimulate bone resorption, e.g., RANK/RANKL/OPG cascade in advanced breast cancer.⁵ Tumour–bone interactions play a fundamental role in therapeutic design, but the crosstalk between cell components varies between patients with the same disease. Remodelling can be affected by various mechanical and molecular stimuli because of ethnic differences, aging, menopause, type and duration of their typical physical activity determine variations in response to different drugs.^{6–8} Additionally, in some cases, such as in



Jacek K. Wychowaniec

Dr. Jacek K. Wychowaniec received his Ph.D. degree in Nanoscience in 2017 from the University of Manchester, United Kingdom. From 2018–2021 he was a Post-Doctoral Research Fellow at the School of Chemistry, University College Dublin, Ireland. In 2021, he successfully secured a Marie Curie Research Fellowship at the AO Research Institute (ARI) in Davos, Switzerland, as a member of the Biomedical Materials group,

where he currently remains a Research Scientist. With a decade of interdisciplinary research experience in different countries, Jacek specializes in combining physical chemistry and bioengineering to develop innovative biomaterials for the next generation of treatments targeting musculoskeletal tissue regeneration. His work has resulted in 51 peer-reviewed publications, and his expertise lies in translating and linking the fundamental behaviour of biomaterials toward desired biological functions.



Carlos A. Villacis-Aguirre

Carlos A. Villacis-Aguirre is a Biotechnology Engineer. He is a PhD candidate in Molecular Biotechnology at the Universidad de Concepción. He has experience in the development of nanomaterials, production of recombinant biopharmaceuticals, and its encapsulation through electrospinning and electrospraying methods for pharmaceutical development. Currently, his work is focused on mRNA vaccine technology.



Matteo D'Este

Dr. Matteo D'Este earned his PhD in Chemistry from the University of Padova in 2006. He has since worked in the pharmaceutical and medical devices industry, focusing on biopolymers and their derivatives. In 2011, he joined the AO Research Institute Davos, where he is now Principal Scientist, specializing in biopolymers, biofabrication, immunomodulatory biomaterials, and drug delivery. Dr. D'Este has

authored six patents and over 70 papers. He is also an adjunct professor at Laval University, Canada, and served as Chair of the 2023 European Society for Biomaterials Conference.



Jorge Toledo

*Prof. Jorge R. Toledo is a microbiologist, with his research focused on molecular biotechnology for the development of new products and services to make an impact on human health. He puts special emphasis on *in vivo* testing for biomedical applications. He has been awarded with more than 30 grants to assess new vaccine candidates, biosimilars/innovative biopharmaceutical infrastructure development and recombinant proteins. Currently, he is Department Director as well as Director of the new Tissue Engineering Unit at Universidad de Concepción.*



advanced breast cancer with bone metastases, there is an epithelial to mesenchymal cell transformation with multiple genetic mutations since the first anatomy-pathology diagnosis (*i.e.*, Goldie–Coldman hypothesis), causing patient-dependent tumour heterogeneity.⁹ The variability between patients influences the prognosis of cancer; therefore, it is mandatory to adapt therapies to the individual characteristics of patient to improve the overall effectiveness.

In the drug development process, more than half of all drugs fail phase II and phase III clinical trials due to lack of efficacy, and about another third fail due to biosafety issues, with an average investment ranging from \$161 million to \$4.54 billion, and between \$944 million and \$4.54 billion for anticancer drugs.^{10–12} The biotech industry has improved several techniques once the effectiveness of a new compound has been demonstrated *in vivo*, generally with rodent models;^{13–15} however it is difficult to homologate the same action in patients due to the variability in the intracellular pathways of the second messenger, as well as drastically different immunological responses in rodents compared to humans.^{16,17} Existing high-throughput screening (HTS) techniques are mainly based on monolayer cell cultures (2D), which significantly differ from the three-dimensional (3D) human extracellular matrix.^{18,19} 2D biochemical and gene expression assays do not achieve adequate predictions when they are employed on the function of genes at the posterior level of a tissue or organ.¹³ The need to improve current methods of developing drugs against bone diseases, such as bone tumours and metastases, is imperative, as current *in vivo* and *in vitro* models have not demonstrated the necessary effectiveness and reproducibility validation.^{14,17}

Innovative cell and tissue-based platform systems that can better resemble human physiological behaviour coupled with emerging assay technologies have resulted in improved models that can change the drug discovery/development process. The simultaneous employment of patient-derived cells, 3D cell culture models, bioprinting, microfluidic devices and automation can bring new chances for succeeding in drug discovery associated with bone diseases.¹⁸ Although a starting point for developing innovative bone models is the selection of scaffold(s) for the 3D cell culture that can resemble the native extracellular matrix (ECM) of the bone tissue, alongside the system that can provide the mechanobiological environment that imitates the biomechanical stimuli present in the bone. The present review aims to provide state-of-the-art summary about existing bone models focused on microphysiological systems (MPS) and to describe strategies to design large-scale assays for mimicking bone environment for studying the influence of novel diagnostic/therapeutic candidates to treat different bone diseases.

2. Bone tissue structure and physiology

Bone is a connective tissue derived from two primary germ layers of the embryonic development. The craniofacial vault and face are derived from the neural crest of the ectoderm and

the remaining long bones come from the mesoderm, which results in meaningful differences in their formation and mineralization processes in the presence (long bones) or absence (craniofacial) of a transitional cartilage template. Bone tissue is characterized by the presence of a highly hierarchical structure composed of assemblies of organic protein and mineralized matrix of mainly type I collagen with a mineral phase of calcium phosphate-based hydroxyapatite (HA) crystals.¹⁹ The composition of different matrices and their anatomical structure vary depending on skeletal site, age, sex, physiological function and mechanical loading²⁰ due to the fact that it has an adaptation capacity modelled by its mechanical environment that causes a fluctuating reordering of its internal basic building blocks²¹ or as unit parts of the hierarchy, *e.g.*, osteon (Fig. 1A). Bone ECM is composed of an organic matrix (30% of bone-dry mass approx.) mainly containing type I collagen fibres (90% of the organic matrix approx.), which forms an interlinked architecture that gives bone its strength and resistance.¹⁹ The non-collagenous proteins include osteocalcin, osteonectin, osteopontin, and bone sialoprotein, allowing the junction of minerals, orchestrating bone mineralization, and regulating bone cell activity in general. Proteoglycans, which are other key components, retain water within the matrix and contribute to the bone's compressive strength and elasticity. Most bone dry mass is composed of an inorganic matrix (70% of bone mass approx.) containing HA crystals that are calcium phosphate ($\text{Ca}_{10}(\text{PO}_4)_6(\text{OH})_2$) minerals, which provide compressive strength and hardness to bone. Other ions such as magnesium, fluoride, and carbonate also contribute to the bone matrix, influencing properties such as strength and density.¹⁹

Bone has two main histological matrix division separated by function, while the cancellous bone is less compact and with irregular shapes containing bone marrow and progenitor cells. Cortical bone has higher mechanical properties and it is responsible for body support due to its mechanical arrangement, which allows to support certain amounts of stiffness. This produces high variations in elasticity modulus and ultimate strength (strength in the range of 5.3–193 MPa and elasticity in the range of 0.4–17 MPa).^{24–26} Trabecular bone is found inside cortical areas and its functional unit is the trabecula that aligns according to mechanical load.²⁷ The marrow is also located within cortical areas; it is highly vascularised and composed of yellow inactive fat marrow and red active hematopoietic marrow that provides stem cell populations for hematopoietic, stromal (connective tissue) and endothelial purposes.²⁸

The outer surface of cortical bone is covered by the periosteum, an innervated and vascularized fibrous membrane, and the inner face is covered by the endosteum that faces the bone marrow. Bone tissue basic functional unit is the osteon, *i.e.*, Haversian system, a structure between 100 and 200 mm (ref. 19 and 27) oriented in a “fractal-like” arrangement of many layers of concentric lamella (3–7 μm thick) that surrounds resident cell osteocytes (90% of total bone cells and about 25 000 osteocytes per mm^3 of cortical



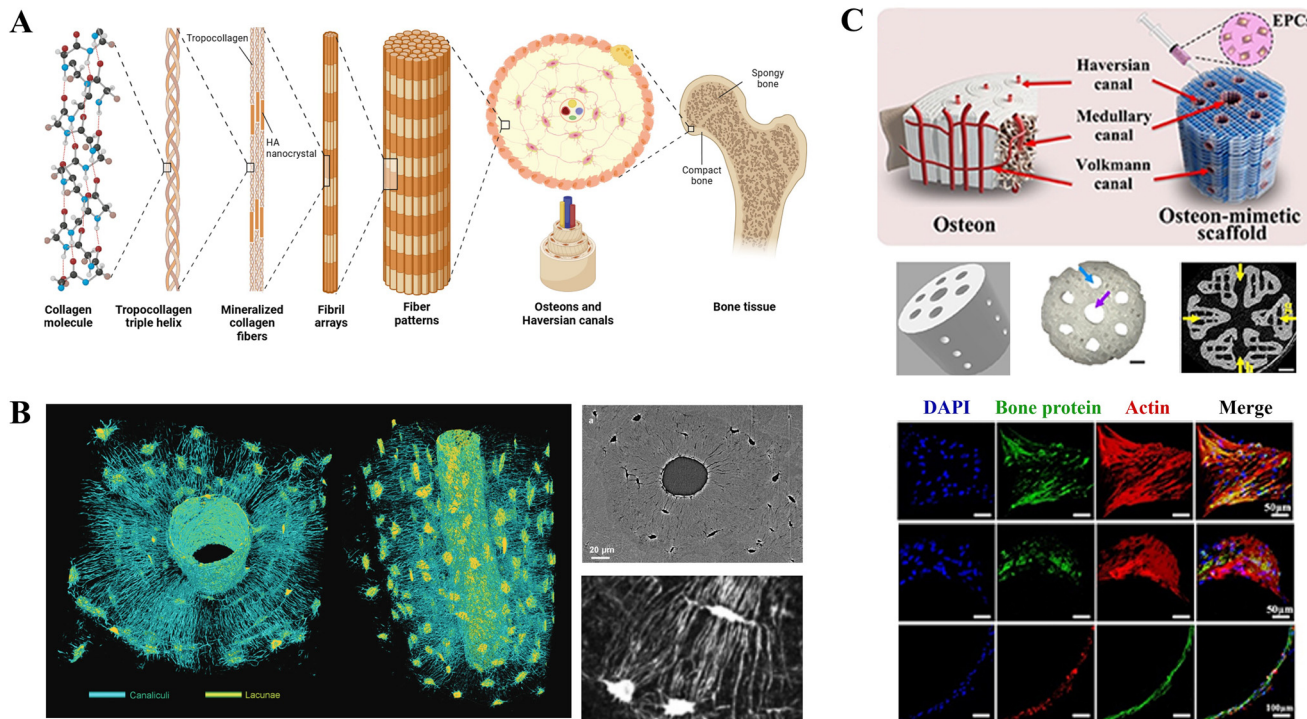


Fig. 1 Schematic of bone architecture and current bone biofabrication capabilities, showing lateral and transversal views and depicting required arrangement that can be replicated by scaffolds and biomaterial engineering. **A.** Levels of hierarchy of bone tissue. Created with <https://Biorender.com>. **B.** Nanoscale spatial resolution of synchrotron imaging of bone and imaging 3D reconstruction for lacunocanicular network in a three dimensional analysis.²² © 2021 John Wiley & sons, Inc. **C.** Bone biofabrication by bioprinting of polycaprolactone bioink with a scaffold design of osteon-mimetic including bone marrow and endothelial cells in the process and confirmed of cell-laden protein-derived matrix deposition of osteopontin, Runx-2 and VE-cadherin.²³

bone) (Fig. 1A). Osteocytes are bone resident cells that are interconnected by canals, *i.e.*, canaliculi. These cells can live up to 25 years and oversee ECM mineral regulation. The circular fashion of secondary (remodelled) osteons, about 50 to 90 μm in diameter, are in the order of blood vessel disposition that are located concentrically to a central vascular channel. This nutrient supply is complemented by the Volkmann channels that interconnect the main vessels.²¹ The osteon (Fig. 1C) in a single case of a single section of cortical bone has areas within that are highly variable,²⁹ and Haversian canal sizes are much more variable than osteon size, though several measurements in humans have estimated a diameter from 200 to 260 μm.³⁰

In the hierarchy of bone (Fig. 1A), the building blocks start at the nanoscale with mineralized collagen fibrils (100 nm in diameter and 5–10 μm in length).^{31,32} These fibrils are composed of several collagen molecules that self-assemble into ordered fibrils to be later covered and compiled between each other with HA crystals (thickness of 1.5–4.5 nm), causing the growth and mineralization of fibrils in a “repeated and staggered pattern”.^{31,32} The osteon arrangement of building blocks at different length scales forms a hierarchical structure that controls its mechanical properties^{22,33,34} and is correlated with different mechanisms of fracture resistance: bone nanostructure allows molecular uncoiling of collagen molecules, mineralized collagen fibrils

sliding to provide collagen fibres bridging, and at the microscale, ligament bridging and crack deflection twist by osteons in the osteo/matrix interface.²¹

Bone has a well-known self-repair capacity that is efficient in the removal and replacement of damaged materials^{35,36} due to its cellular content in a period that lasts 120–200 days in the case of cortical bone.³⁷ The cell sources in bone are osteoprogenitor cells, osteoblasts, osteoclast and osteocytes.³⁸ The mineral matrix surrounds the osteocytes cells, while osteoblasts and osteoclasts are in zones of bone remodelling that allows structural adaptation to functional external requirements and repair.^{21,35,36} The osteoblasts are derived from mesenchymal stem cells (MSCs) or precursors and responsible for mineralized matrix deposition. Once surrounded by the matrix, they become osteocytes in a space call “lacunae”. The “damaged or old” bone removal is maintained by multinucleated cell hematopoietic precursor-derived osteoclasts with mineralized bone resorption.³⁹ All these cell sources maintain bone homeostasis by active crosstalk regulated by two proteins, the receptor activator for nuclear factor κB ligand (RANKL) and osteoprotegerin (OPG).⁴⁰ The dynamic process of remodelling, orchestrated by the cell components, changes depending on the mechanical load induced by strain and interstitial fluid flow,⁴¹ which cause the hierarchical growth of the microstructure adaptable for optimizing its structure under specific functions.^{42–44}

Bone ECM has been increasingly more important subject to active research since 1950. In the last decade, this has come for its relevance in the fields of tissue regeneration and disease modelling, which employ novel biomimetic designing and biofabrication strategies (Fig. 1C).²³ The different states of bone make it a dynamic tissue with several different features depending on personal characteristics and disease. The bone matrix is a dynamic tissue able to produce different types of bone structures with modifications in cortical and medullar length, mineral, cell density and biological activity phases depending on environmental and individual characteristics. With the aging process, the changes in the bone ECM cause and maintain several diseases with deep local implications that can cause fragility and bone fractures, with high association between femoral fracture and age.^{45–50} Moreover, there are several common bone pathologies^{46–60} that have reported ECM changes with clinical implication (Table 1), such as the case of secondary bone metastasis from breast and prostate cancer that are usually characterized by an altered and increased state of bone remodelling process

with bone loss replaced by malignant tumour cells increasing the chances of pathological fractures.

3. *In vitro* bone models

Cells and tissues can be studied for tissue regeneration, precision medicine and novel biomarkers to acquire new and improved preclinical models that resemble human biology. The reproducibility of *in vitro* models by tissue engineering is a major advance that may enable improved success rate in pharmaceutical development and *in vitro* diagnostics.^{61–63} Hence, the selected cell source should behave as in the human body, and it is necessary to provide the appropriate mechanical cues from the ECM for accomplishing critical reproducibility of the *in vivo* experiments. In the 1980s, Bissell's group established the importance of ECM components in cell behaviour,⁶⁴ and nowadays, it is well-known that 3D cell culture mimics tissue in a way that is much more representative of the *in vivo* environment than traditional 2D cultures.^{65,66} Although the standard method is

Table 1 Specific signs and ECM characteristics of different bone diseases

Disease	Description	ECM characteristics	Ref.
Osteopenia	Low bone mass and low bone mineral density Higher risk of developing osteoporosis	The intracortical porosity is increased with age, and advanced age is strongly correlated with decreased osteocyte lacunar density (less osteocyte cells)	45, 46
Osteoporosis	Skeletal disorder characterized by compromised bone strength, leading to an increased risk of fracture Bone mass reduction and alteration of bone architecture	The trabecular bone matrix mineralization is reduced; there are alterations in collagen alignment Increasing age causes a decrease in the total protein phosphorylation levels, 20% approx. for bone matrix proteins and approximately 30% for osteopontin Reduction of bone matrix with thinner trabecular areas, microfissures, enlargement of medullary spaces of the bone and increased adipose degeneration of the marrow	47–50
Osteogenesis imperfecta	The “brittle bone disease”, genetic disorder characterized by a decreased bone density with increased risk of bone fractures Mutations in the COL1A1 or COL1A2 genes are associated with abnormality in the synthesis and/or processing of type I collagen, as in the bone architecture	Mineralization is increased, although there is an altered bone ECM formation and structure. Lamellae are present with irregular organization and a mesh-like appearance There are significantly smaller, highly packed, and disoriented apatite crystals ECM with lower stiffness and elasticity Histopathology shows a high increase in cortical porosity, canal diameter, and connectivity	51–54
Osteosarcoma	Neoplastic transformation of bone cells. Commonly, osteoblastic-derived subtype These lead to decreased bone strength and can cause pathological fracture by minor trauma	ECM transformation with a robust ECM with pathogenic osteoid matrix The osteosarcoma ECM is a scaffold for rapid tumor progression, rapid bone resorption and deposition Presents a disorganized alignment and increased isotropy in porosity and collagen fibers Many ECM proteins, such as collagens I, III, IV and V, fibronectin and laminin. Other proteoglycans are increased in the ECM	55–57
Secondary bone metastasis	Depending on the primary tumour, e.g., breast and prostate Commonly lead to sudden noticeable new pain and may lead to predisposition to bone fractures	There is a skeletal phenotype of disorganized collagen microarchitecture, abnormal arrangement of osteoblasts and apatite crystals Increased osteolytic activity produced by secondary tumors cause an accelerated bone turnover with less stiffness (14% lower Young's modulus) and more brittleness than normal lamellar bone	59, 60



still the most widely used for HTS assays, 3D cell culture is increasingly being employed.^{67–70} Protocols involving 3D cell culture allow the formation of multicellular tissues with better cell–cell and cell–ECM interactions that can mimic the physiological processes of tissue expansion, function, and differentiation. The use of 3D cell models for the study of disease progression *in vitro* is particularly useful when there are abnormal tissue organizations with changes in the ECM composition (e.g., fibrosis, solid cancers or osteoporosis).^{71–73} For example, there are major morphological changes that occur when cells (both primary and cell lines) are cultured in 2D *vs.* 3D⁷⁴ and when different 3D scaffolds are used for imitating the extracellular matrix. These can result in several molecular pathways modified with impact on osteoconductivity and mineralization capacity.⁷⁵

An ideal 3D cell culture model is the one that generates a physiological and/or pathophysiological microenvironment of a specific tissue tuned to a specific disease and thus enables cells to proliferate, aggregate and differentiate in a niche-specific manner. These 3D models enable cell–cell–ECM interactions, granting a specific rigidity with gradients of oxygen, nutrients, and metabolic waste typical of the tissue to be studied.⁷⁶ When scaffold-free “spheroid” organizations are used (Fig. 2), they do not meet the criteria of an ECM without mimicking cell and tissue-specific polarity, but they can develop metabolic gradients that create heterogeneous cell populations with cell-to-cell interactions, and they are easier to produce and handle for HTS. This easy-handling approach has been employed for bone developmental studies and bone healing,^{77,78} especially when human umbilical vein endothelial cells (HUVEC) are used in a co-culture setting,^{79–82} demonstrating a useful platform for replicating physiological processes. Unlike 3D models with scaffolds or “organoids” that better mimic *in vivo* conditions thanks to the use of a biomaterial or scaffold where cells are encapsulated, an adequate microenvironment for their polarity, migration, growth, and interaction can be provided to achieve mini-organs or mini-tissues (Fig. 2).

For years, 3D cell culture focused on using hydrogels derived from basement membrane extractions of animal origin (e.g., Matrikel derived from Engelbreth–Holm–Swarm mouse sarcoma cells), permitting the growth of cells that are otherwise difficult to culture, such as primary cells. Although they have relatively stable properties, they have highly variable batch-to-batch composition, making the reproducibility of assays difficult and often unstable.⁸³ To overcome this obstacle, synthetic biomaterials have been proposed as a solution for accurate batch-to-batch reproducibility and possible customization.⁸⁴ However, most pure-synthetic scaffolds lack ECM proteins, which limits the physiological relevance of single synthetic component substrates at the level of cell anchorage and interaction.¹⁸ Cells cultured on inert hydrogels or purely synthetic scaffolds can grow with low adherence, and they do so through the secretion of endogenous ECM proteins or because of oncogenic mutations that confer anchorage independence.⁸⁵ Therefore, the strategy of using hybrid matrices that combine synthetic and organic biomaterials for improving cell adhesion and mechanical stimuli and/or sensing has expanded,^{86,87} in addition to the use of these platforms with different cell types such as osteoblasts and osteoprogenitor cells capable of synthesizing new ECM.^{88–90}

Overall, 3D cell culture strategies for designing new preclinical bone-related models must consider the challenges associated with the high costs of scaffolds biomaterials (e.g., Matrikel),⁹¹ assays that require penetration and interactions of markers into the gel (e.g., antibody staining), adjustments in viscosity and gelation that is sensitive to temperature, causing difficulties in the automated handling of HTS.^{92,93} However, the integration of different design strategies complemented with HTS and automation technologies (e.g., bioprinting and instrumented liquid handling) can generate improved assays with greater reproducibility and physiological similarity.^{94–96} In the next sections, we will provide prominent benchmark work leading towards the generation of reproducibility and model validation.

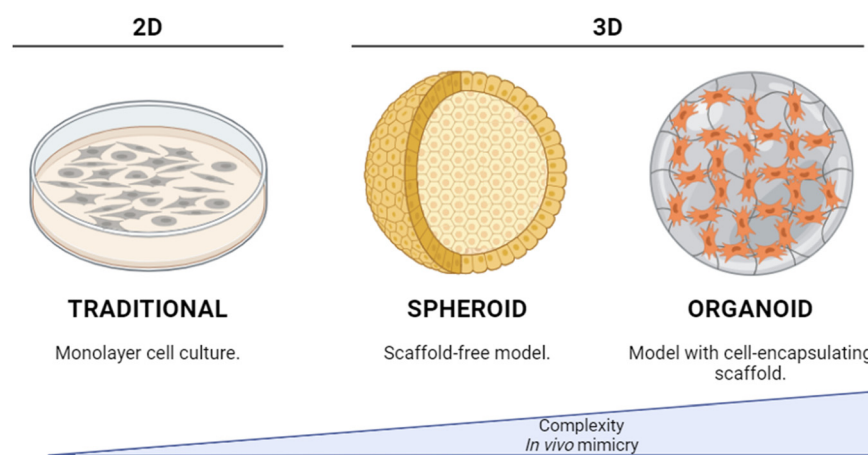


Fig. 2 2D vs. 3D (spheroid or organoid) cell culture approaches. The major points describing each approach are noted below. Created with <https://BioRender.com>.



4. Extracellular matrix for bone bioengineering

In 3D cell culture, the most common strategy to bioengineer or create artificial bone *in vitro* involves combining an ECM (or scaffold) with a bone-focused cell source. This process is carried out in either a static system (e.g., T flasks) or a dynamic system (e.g., bioreactor) under physiological temperature and humidity conditions for a period of time. The biomaterial supports cell differentiation, proliferation, and migration, thereby emulating the *in vivo* conditions to some extent.⁹⁷ To achieve a representative bone model, the selected scaffold should mimic the bone ECM, complying with the following: (i) biocompatibility, (ii) facilitate cell differentiation and proliferation, (iii) close to natural biomechanics, (iv) a porous structure that allows cell reorganization, promoting angiogenesis and (v) adequate biodegradability to promote remodelling^{98,99} (Fig. 3). Biocompatibility is the fundamental characteristic for the support of bone-cells activity in a physiological manner. The other key feature is osteoconductivity, and the capacity to facilitate bone growth, positively influencing cell adhesion, proliferation, and bone ECM deposition.^{100,101} Osteogenicity is essential to promote bone differentiation in bone-cells, such as osteoblastic-related cell lines, osteoprogenitor cells, and MSCs. This property is modulated by the cell-ECM interaction.¹⁰² At the same time, the appropriate design of a scaffold with the same mechanotransductional signals to bone is required.^{103–105} Biodegradability plays a key role in bone engineering and its rate must be inversely proportional to the bone deposition rate to mimic natural bone physiology.¹⁰⁶ This rate is dependent on the scaffold characteristics (e.g., chemical composition,

microarchitecture and mechanical properties), physicochemical microenvironment (e.g., temperature, pH, O₂ and CO₂) and biological factors (cell source and composition of chosen cell culture medium).^{17,107–109} The porosity is 50 to 90% in spongy bone and 3–12% in cortical bone. This low porosity in an osteon arrangement makes cortical bone much more resistant.^{110–113} It has been previously described that a minimum pore size of 120 to 325 µm in diameter is required to induce ossification and subsequent oxygen supply under hypoxic conditions.^{110,114}

Bone cells, such as resident osteocytes, attach to a scaffold primarily by integrin receptors on their cell membrane. These receptors can bind to short peptide arginine–glycine–aspartic acid (RGD) motifs, which are present in the ECM proteins, including collagen type I, laminin, and fibronectin.¹¹⁵ These motifs also repeat in denatured collagen, *i.e.* gelatin. Hence, one of the common strategies is to chemically decorate the scaffolds' surface with RGD motifs to promote attachment and enhance cell–substrate interactions through integrin binding.^{116–118} RGD peptides are well-known molecules used for enhancing the initial adherence of osteoblastic and other cell lines (e.g., SaOS-2 and MC3T3-E1) on tissue-engineered matrices based on synthetic degradable polymers. A comparison study was performed between RGD and RGE motif, where aspartic acid was replaced by glutamic acid, making the RGE motif unable to bind to integrins. Consequently, 3D cell culture with MSCs demonstrated that RGD hydrogels were highly superior in cell attachment, viability and osteogenic differentiation as compared to the RGE hydrogel group.¹¹⁹

Bone has an established structural hierarchy in the nano/micrometric range,^{71,77} and it is possible to provide a similar niche compared to the bone ECM through scaffold micro/nanostructure modifications. These could mimic bone tissue topography, hence promoting the osteogenic differentiation of MSCs.^{120,121} In order to resemble the ECM by scaffolds, some groups have been able to direct specific osteogenesis and osteoclastogenesis responses by incorporating osteon-like concentric microgroove patterns on the surface of scaffolds.^{44,122} Biofabrication techniques can also be used to control the uniformity of cell distribution or cell localization on the surface of a scaffold,^{123–125} to incorporate bioactive molecules^{44,126} and for controlled therapeutics delivery purposes.^{127,128} The effects of material sizes have been elucidated across multiple length scales (from mm towards nm), and it has been reported that nanostructured biomedical implant surfaces can trigger osteogenesis by targeting osteoblasts, osteocytes and MSCs.¹²⁹ For example, studies have demonstrated that emulating the ECM through calcium phosphate-based concave discs with varying concavity sizes (440, 800, or 1800 µm) exhibit distinct osteogenic outcomes when MSCs are used. Notably, 440 µm concavities showed enhanced cell proliferation and superior osteodifferentiation potential, as evidenced by the upregulation of osteocalcin mRNA compared to larger concavities (800 and 1800 µm) at the microscale,¹³⁰ which was putatively assigned to increased cell proliferation in smaller concavities. This study highlights the ability of MSCs to sense and respond to the geometrical

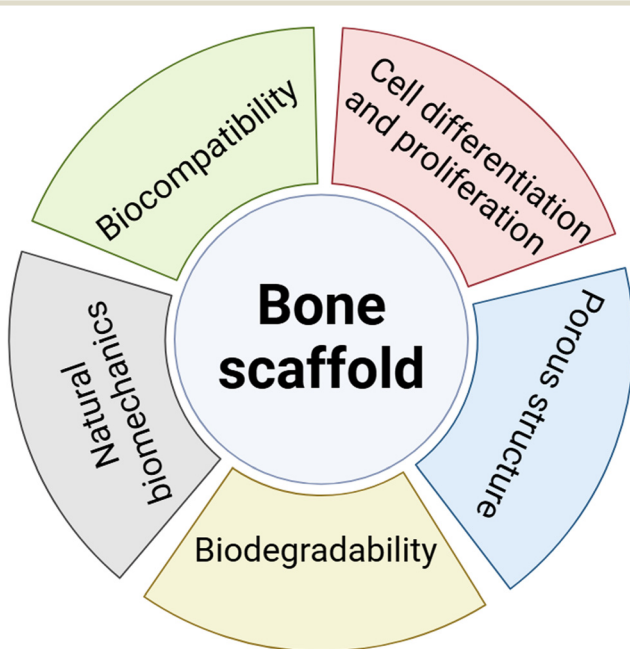


Fig. 3 Bone scaffold considerations for the mimicry of ECM by a scaffold. Created with <https://BioRender.com>.



properties of scaffold surfaces, influencing their organization and osteogenic gene expression, mimicking the effects of ECM changes in response to different disorders and diseases. Similar findings of best differentiation were also found at the nano- and micron-scale (0.2–2.4 μm) with human adipose-derived MSCs on polymer titanium nanotubes surfaces.¹³¹ The TiO_2 nanotubes effect was evaluated by transcriptomics, indicating that cells seeded on TiO_2 nanotubes were more spread out with longer and netted pseudopodia, resulting in cytoskeleton reorganization with forces transmitted to the nucleus *via* physical links of laminin on the nuclear envelope.¹³¹ Noteworthily, the anisotropy of the bone structure is determined by how cells deposit the ECM in concentric lamellae in a certain concentric order^{114,120} (Fig. 1). It was demonstrated by polymethylmethacrylate lithography-generated scaffolds that highly ordered nanotopographies produced low cell adhesion and poor osteoblastic differentiation of MSCs and that cells in random design between 20 and 40 nm generated osteoblastic morphology with raised osteopontin and osteocalcin expression, even in the absence of osteogenic supplements in medium during 28 days of culture.¹²⁰ The insights gained from this study may indicate that *in vivo* ECM is inherently heterogeneous, and cells are biologically programmed to thrive in environments that mimic this complexity, unlike highly ordered topographies that may appear “unnatural” to cells. For more description of topographic strategies for designing scaffolds, we refer readers to ref. 132 and 133, and specifically for bone to ref. 134 and 135.

The mechanical stiffness of the scaffold must mimic the same human bone stiffness and matrix architecture that resembles bone. This however varies depending on the process to be emulated, spanning from physiological remodelling in bone repair and regeneration (Table 2). In the year 2006, Engler *et al.*¹³⁶ identified the elasticity of the matrix microenvironment as a key regulator for the lineage of stem cell fate and provided evidence that when changes in the stiffness of the substrate occur, MSCs could be directed into bone lineages. Using atomic force microscopy (to identify the material's resistance to local deformation when subjected to an indentation force), they measured the ECM deposition and osteoid of human osteoblasts after 7 days of culture on a glass 2D surface, resulting in a stiffness of 27 ± 10 kPa. This range was later simulated with polyacrylamide gels (stiffness of ~ 34 kPa) as the substrate for MSCs, which were able to express bone lineage by upregulating osteocalcin and the early transcriptional factor RUNX2 (*i.e.*, CBFa1). Although the indentation modulus differs from an extensional modulus that measures the entire structure, this was an important first approach for revealing key points of stiffness and osteogenic expression. Hence, it seems that the stem cell niche is crucial for the osteogenic-lineage differentiation of MSCs through the substrate stiffness and topography. In a study by Li and colleagues,¹³⁷ these three features were combined for evaluating bone marrow MSCs (BM-MSCs) responses by different concentrations and topographical geometry of polyacrylamide gels. They reported that a specific 3D substrate is crucial for guiding BM-MSCs osteogenic differentiation, establishing that for scaffold design and selection, substrate stiffness was a more

relevant feature than topography for proliferation and differentiation. Specifically in osteogenic lineage, they observed higher expression of RUNX2 and $\beta 3$ -tubulin when the cultures were in the 25–40 kPa stiffness range.

Table 2 presents an exemplar list of studies that show the influence of material stiffness on the final fate of the fabricated bone, selected examples of which are discussed in the text.^{114,136,138–143} The characteristics of resistance to compression, stiffness, and elasticity vary significantly between cancellous and cortical bone, and these change during repair and remodelling phases. In terms of biomechanical differences, most studies employed either the bulk extensional modulus or microscopic local indentation technique, and one literature review mentioned some variations depending on the test used. Briefly, cortical bone from femoral heads have been reported to have an elastic modulus of 18 ± 1.8 GPa and 153.5 ± 21.6 GPa of ultimate stress measured by compression loading.¹³⁸ On the other hand, cancerous bone is much more difficult to estimate as it is much more active and dependent on individual and external factors (elastic modulus values in the 1–22.3 GPa range were reported).¹³⁹ Huebsch *et al.*¹⁴⁰ cultured murine MSCs in composite hydrogels made of alginate, agarose, and peptides with elastic modulus in the range from 2 to 110 kPa and found that the best osteogenic commitment was present in hydrogels with moduli in the 11–30 kPa range. Also, Olivares-Navarrete *et al.*¹⁴¹ demonstrated that MSCs are capable of osteogenic differentiation, depending on substrate stiffness. Without exogenous growth factors, they cultured human MSCs on the surface of methyl acrylate (MA) and methyl methacrylate (MMA) crosslinked with 10% poly(ethyleneglycol) dimethacrylate (PEGDMA) hydrogels. They compared the responses of hMSCs with human osteoblasts and found that the highest RUNX2 levels on gene expression were seen on softer surfaces (*i.e.* 0.8 ± 0.1 MPa) in both cell types and that MSCs were more sensitive to stiffness than osteoblasts. Surprisingly, this study revealed that stiffnesses in the range 40 MPa were better for inducing osteogenic differentiation from MSC, way below the maximum tested stiffness of 72 MPa. Zhang *et al.*¹⁴² bioprinted cell-laden 3D bone-like engineered constructs by the combination of alginate and gelatin hydrogels with human MSCs (hMSCs) at a density of 5 million cells per 1 mL ink solution in two main formulations (elastic modulus of 1.8% alginate: 750 ± 81 Pa and 0.8% alginate: 484 ± 46 Pa). After 3D culturing in osteogenic media for 42 days, their findings were significantly different from most other studies, *i.e.*, softer scaffolds induced better hMSCs proliferation, enhanced osteogenic differentiation and significantly higher HA-like mineral formation compared to stiffer scaffolds. This was most likely due to softer scaffold allowing more cell spreading and facilitating easier cell-mediated degradation for higher cell spreading degrees. The summary of scaffolds presented here extends the understanding of how to mimic bone ECM and highlights their potential applications in designing experiments involving 3D bone cell cultures.



Table 2 Bone model features for designing a bone scaffold

Study feature	Substrate characteristic	Main findings	Testing technique(s)	Ref.
ECM composition and micro-indentation properties	Femoral head axial plane strain modulus (GPa) Osteonal: 18.09 ± 1.73 Interstitial: 13.10 ± 1.94 Tension: 18.16 ± 1.88 Compression: 18.97 ± 1.84	Porosity was directly linked to the macroscopic tensile, compressive and torsional mechanical properties of human cortical bone	Local indentation, microindentation and mechanical testing	138
Review of Young's modulus of trabecular bone	Range from 1.2 to 22.3 GPa	The stiffness of bone varies due to bone heterogeneity, geometry, hierarchical structure and mechanical testing	PubMed bibliographic database review	139
Influence of microenvironment stiffness on stem cell specification	Polyacrylamide gels: 0.1–1 kPa, 8–17 kPa and 25–40 kPa	MSCs can be directed to an osteogenic commitment	Local indentation Atomic force microscopy	136
Commitment of MSC in response to the rigidity of 3D micro-environments	Engineered hydrogels (alginate, agarose and peptides) in the range from 2 to 110 kPa	Osteogenesis occurring predominantly at 11–30 kPa	Extensional modulus (mechanical instrument)	140
The role of stiffness in MSC osteogenic differentiation	Methyl acrylate (MA) and methyl methacrylate (MMA) crosslinked with 10% poly(ethylene glycol) dimethacrylate (PEGDMA) % of MA (MPa): 18MA (309 ± 6.5), 29MA (223.7 ± 31.5), 40MA (4.7 ± 1), and 72MA (0.8 ± 0.1)	Stiffness can direct the osteoblast fate of MSCs; afterwards, stiffness has different effect, suggesting that softer substrates could halt further osteoblast maturation	Extensional modulus (mechanical instrument)	141
Cell-laden 3D bone-like engineered constructs	Alginate and gelatin hydrogels: 1.8% alginate: 750 ± 81 Pa. 0.8% alginate: 484 ± 46 Pa	Softer scaffolds result in better osteogenic differentiation, and a lower cell density can promote a higher mineral formation rate (5 M cells per mL vs. 15 M)	Extensional modulus Rheometer	142
Effect of pore size on bone tissue engineering	Lyophilized of collagen-glycosaminoglycan scaffold	MSCs attachment and osteocalcin expression are increased in larger pores (325 μ m)	Optical microscope	114
3D microstructure with tuneable mechanical properties	Mixtures of collagen and hydroxyapatite ranging in stiffness from 6.74 ± 1.16 kPa to 37.7 ± 19.6 kPa	Stiffer scaffolds enhance osteopontin and osteocalcin deposition <i>in vitro</i> and <i>in vivo</i>	Local indentation Atomic force microscopy	143
Bone-like tissue model encompassing mineralization, vasculature, innervation and prostate cancer coculture	Mineralized hydrogel constructs of the order of 20 GPa	Tumor growth kinetics was significantly higher in mineralized samples than in non-mineralized controls after <i>in vivo</i> subcutaneous implantation	Local indentation Atomic force microscopy	144

5. Bone-on-a-chip

MPS known as organ-on-a-chip (OOC) technologies are a new approach to mimic miniaturised human tissues or organs, tissues interfaces and multi-organ systems as physiologically-relevant testing platforms, and several reviews have already been published.^{137,145–147} OOC platforms have the great advantage of recreating the human physiological relationship between tissues and organs in a “vasculature-like” system in the presence of microfluidic channels and compartments capable of reproducing physiological cues similar to those of human organ functionalities, such as pharmacodynamics (PD) and pharmacokinetics (PK) effects of drug candidates. The chips can be designed with optically clear plastic, glass or

polymers (e.g., polydimethylsiloxane, PDMS), which contain microcompartments to deposit the living microtissues and hence recapitulate *in vivo* functions by interconnecting them. Fabrication of these devices can accomplish complex designs by connecting different compartments with different tissues and organ cell types constructs for studying and resembling multi-organ interactions. This can be done with semi-permeable membranes to maintain the tissues in their places, but allowing the perfusion of the culture medium.¹⁴⁸ The presence of these microchannels allow the viability of cells to be maintained for longer periods, even up to months,¹⁴⁹ and allow the employment of relevant human physiological aspects.

Table 3 summarizes multiple OOC approaches for modelling functional bone, highlighting a diversity of cell



Table 3 OOC bone models in non-cancer research

Bone model	Cell types	Mechanical stimulation	Chip material	Scaffold	Ref.
High-throughput efficacy evaluation of biomaterials	Mouse calvarial preosteoblast cells (MC3T3-E1), <i>S. epidermidis</i> strain (NJ9709)	No	PDMS, PMMA cover and ground plates	Biphasic BCP nanoparticles (50:50 hydroxyapatite and tricalcium phosphate) in poly(D,L-lactic-co-glycolic)	151
Osteogenesis comparison of MSCs	BM-MSCs, AD-MSCs	Yes, cyclic mechanical stimulation (1 psi, 1 Hz, 50% duty ratio) for 10 min every 12 hours for 7 days (pneumatic pressure controlled with a switching solenoid valve)	PDMS, PMMA, glass	No	152
Bone marrow haematopoiesis model	<i>In vivo</i> engineering of bone marrow: chip implanted subcutaneously composed of hematopoietic cells and few adipocytes	No	PDMS	Collagen I with demineralized bone powder (mice femur), plus BMP2 and BMP4	153
Vascularized bone tissue model	HUVECs	No	PDMS	Fibrin with hydroxyapatite nanocrystals	154
HTS of bone vascularization variables	hMSCs and osteo-differentiated MSCs (primary isolates) and HUVECs	No	PMMA	Fibrin with collagen (60:40)	155
Bone marrow niche for iPSCs long-term (28 days) culture	hMSC, UC-HSPCs (primary isolates)	No	PDMS, glass	Hydroxyapatite-coated zirconium oxide-based (Sponceram®, Zellwerk GmbH, Germany)	156
Assessment of mechanically regulated osteocyte-osteoclast communication	Osteocyte-like MLO-Y4 cells and osteoclast precursors (RAW264.7)	Yes, fluid shear stress 2 Pa (1.65 Pa, 0.28 Pa, and 0.07 Pa)	PDMS, glass	No	157
Mechanotransduction of primary human osteocytes and modelling parathyroid hormone (PTH) treatment	MLO-A5 (post-osteoblast/pre-osteocyte cell line), hOB (primary isolate) and MLO-A5 (osteocyte-like)	Yes, rate of 0.5 mL min^{-1} at a frequency of 0.17 Hz and shear stress by cyclic compressive loading (artery clamp in outlet)	PDMS, polyester membrane	Bi-phasic calcium phosphate microbeads (20–25 μm in size) (68% of hydroxyapatite and 32% of β -tricalcium phosphate)	158
Rheumatoid arthritis disease model	Fibroblast-like synoviocytes, mouse BM-MSCs, mouse pre-osteoclastic cells (RAW264.7) and human synovial sarcoma (SW982)	No	PDMS, glass	Matriigel	159
Migration evaluation of human osteoblasts on 3D collagen-based matrices	Human osteoblast (HOB, C-12720, Promocell)	Yes, oscillatory strain cycles (0.1 Hz)	PDMS-Dow 35 mm glass-bottom Petri dishes	Collagen type I (BD Bioscience)	160
Investigation of bone-forming cell responses cultured on fibrous collagen matrices	MC3T3-E1 osteoblast-like cells from new-born mouse calvaria	Yes, shear stress (flow rates of 30 and 50 $\mu\text{L min}^{-1}$ were used)	Glass, poly(methyl methacrylate) (PMMA) chips with PDMS gaskets	Collagen type I, rat tail	161
Engineered human vascular marrow niche to examine hematopoietic cell trafficking	HUVECs, stromal fibroblast cell lines HS5-GFP and HS27a-GFP. Peripheral monocytes, mono nuclear cells (primary isolates) and BM-MSCs	No	PDMS	Collagen type I	162



Table 3 (continued)

Bone model	Cell types	Mechanical stimulation	Chip material	Scaffold	Ref.
Investigation of bone remodelling pathways	MC3T3-E1 pre-osteoblasts, RAW264.7 pre-osteoclasts	Yes, strain by applying an out of plane distention to a deformable membrane	PDMS	Bone wafer (6 mm diameter, 0.4 mm thick)	163
3D- <i>in vitro</i> bone model validation w/undifferentiated ADSC	hAD-MSCs, human primary osteoblasts (HOB-C), AD-MSCs, MLOY4 osteocytes	No	PDMS, glass	Collagen type I (rat tail)	164
A co-culture platform to study the interaction between osteocytes and other bone cells	MLO-Y4 osteocyte-like cells	Yes, shear stress by custom in-house pump (0.5 Pa, 1 Pa, 2 Pa)	PDMS	No	165
Innovative living cell microarrays of osteoblasts and osteocytes communication	MLO-Y4 MC3T3-E1 pre-osteoblasts	Yes, fluid flow shear stress (shear stress of 10 dyn cm ⁻² during 15 s)	Sticky microfluidic channel (sticky slide VI ^{0.4} Luer, Ibidi)	Bovine plasma fibronectin (75 µg mL ⁻¹)	150
Lab-on-a-chip platforms for stimulating osteoblasts and quantifying bone remodelling	MLO-Y4 MC3T3-E1 pre-osteoblast, RAW264.7 osteoclast precursor	Yes, physiological (≤10% strain) vs. physio/supraphysiological load (15–19% strain)	PDMS	Collagen type I	166
Organ-on-chip model of trabecular bone	hMSCs from human bone marrow aspirates	No	PDMS	Calcium phosphate, layer coating	167
Microfluidic system for replicating bone sensory innervation	Rat dorsal root ganglion neurons and rat bone marrow mesenchymal stem cells (MSCs)	No	PDMS	No	168
Microfluidic-based neuro-vascularized bone chip model for evaluation of interactions in the inflammatory bone niche	Osteoclasts derived from mice bone marrow, murine embryonic dorsal root ganglia and HUVECs	No	PDMS	Fibrin and collagen type I/fibrinogen hydrogels	169
Multi-sensor (impedance, pH and oxygen) glass-chip for the characterization of cellular behavior	Mouse-embryonal/foetal calvaria fibroblasts (MC3T3-E1)	No	PDMS	No	170
HTS microfluidic platform based preclinical evaluation of drug efficacy	Murine osteocytes MLO-Y4 and osteoblasts MLO-A5 Oc-like cells	No	96 chips (two-lane OrganoPlate® device, 9605-400-B, Mimetas BV)	Matrikel® (Corning) and Cultrex™ (R&D systems), both mixed with rat tail collagen type I at 1:1:8 ratio. Plus, hydroxyapatite nanocrystals (concentration of 0.1–0.2–0.4–0.8% w/v)	171
HTS biomimetic bone-on-a-chip platform for high-content drug screening testing	Mouse osteocytes (IDG-SW3) and osteoblasts (MC3T3-E1)	No	PDMS	Osteoblast-derived decellularized extracellular matrix (OB-dECM, at 1 mg mL ⁻¹) and rat tail collagen type I mixture (2 mg mL ⁻¹)	172



Table 3 (continued)

Bone model	Cell types	Mechanical stimulation	Chip material	Scaffold	Ref.
Real-time morphogenesis evaluation on chip platform with a deep learning platform coupled	Osteoblasts MLO-Y4 cells	Yes, shear stress (30 r min ⁻¹ speed) at different time periods (0, 60, 120, 180, and 240 min)	Not specified	No	173

sources, scaffolds and perfusion techniques employed. Most OOC chips are fabricated using the polymer PDMS, an optically clear and non-toxic silicone polymer, which can be generated by standard or soft photolithography with cell inlet designs to deposit cells or cell on 3D scaffolds by connections such as punch biopsies, syringe needles (around 0.5 mm), optically accessible glass coverslips and waste reservoir for collecting samples (Fig. 4). These kinds of OOCs allow variable mechanical stimulation on the cultured cells by controlled shear stress loading. The effects of perfusion and media content on bone-derived cells, such as osteocytes, can be measured as well as the interactions with other cell types, such as human umbilical vein endothelial cells (HUECs), MSCs and cancer cells. There are some chips with special features, such as the one operated by Yvanoff *et al.*,¹⁵⁰ a sticky bottomless microfluidic chip with 6 channels in a slide for cell

culture applications with a self-adhesive underside to which own substrates can be mounted and where unidirectional laminar flow can be applied to provide homogeneous laminar shear stress in the channels. Such OOC platforms permit cost-effective experiments, reducing the required construct size to fewer numbers of cells, low volumes of materials and reagents such as scaffolds and medium.

Many groups operating OOC have employed protein-based scaffolds, such as collagen,^{160–162,164,166} mainly type I, or fibrin-based gels scaffold,^{154,155} but both lack the mineralized component, *i.e.*, the main bone component. The addition of some form of calcium in the scaffold formulation has been adopted, such as HA and/or calcium phosphate, which may be a useful approach for mimicking bone stiffness and topography as it is 70% of the weight of the human bone mineral.^{123,151,154,167} The use of bone grafts and substitutes,

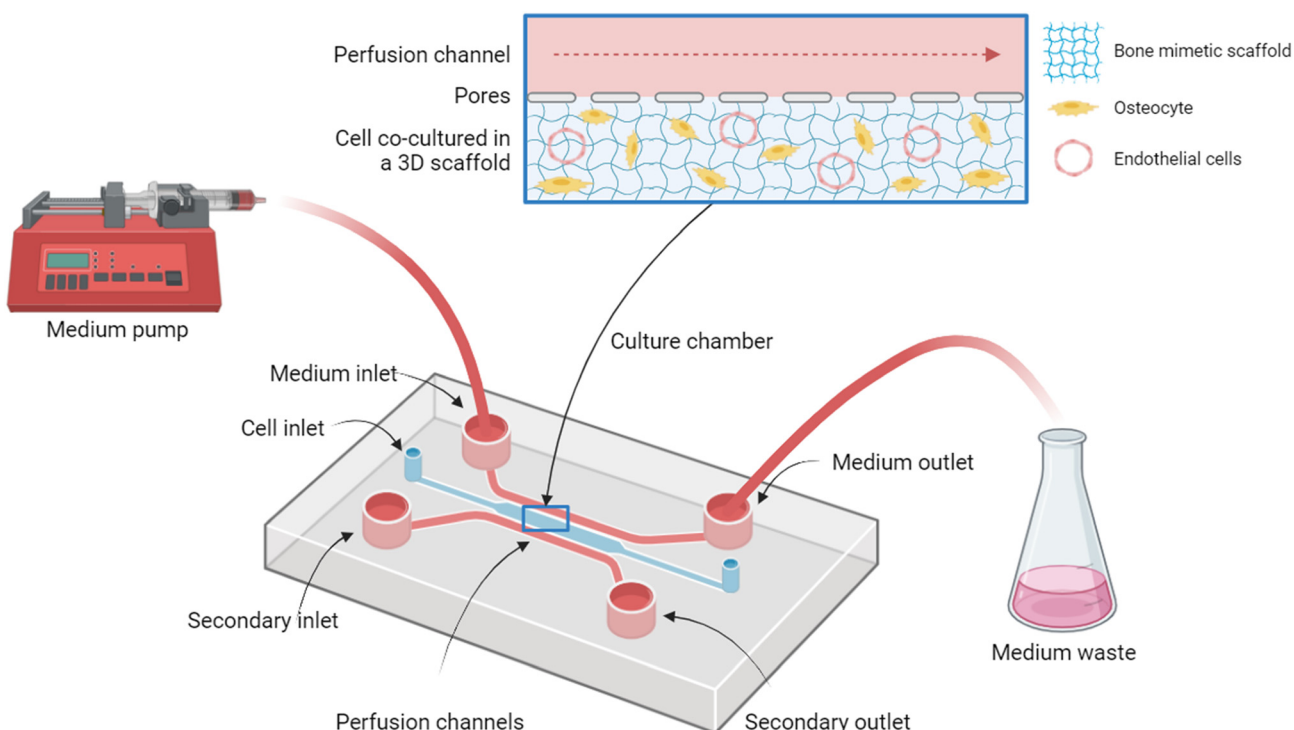


Fig. 4 Organ-on-chip (OOC) basic features. Scheme of a polydimethylsiloxane (PDMS)-based microfluidic culture device with a central perfusion culture chamber for maintaining the 3D cell co-culture; in this case, osteoprogenitor and HUECs are outlined as examples. The perfusion channel is connected to a medium pump, which flows the medium through the microfluidic channel towards a medium outlet connected to a medium waste container. Secondary inlet and outlet can be used for reagent addition and sampling without interrupting the perfusion assay. In the culture chamber, bone-cells, such as osteocytes and vascular cells, can be co-cultured in a 3D bone matrix. The nutrients can be supplied from the perfusion channel by establishing a semi-permeable barrier (as pores) that contains the flowing media culture. Created with <https://BioRender.com>.



already historically successfully used in clinical bone regeneration, as scaffolds for 3D cell culture in OOC systems may offer advantages over single protein-based scaffolds. These are based on real bone (*i.e.*, donated bone) or are based on the mineral content of natural bone tissue (*e.g.*, HA and calcium phosphate), and they provide a more resembling substrate for mechanotransductional signals for the cultured cells that will be attached in it. Some groups have deposited bone grafts in the OOC,^{153,163} and a relevant example of this was reported by Torisawa *et al.*¹⁵³ The group prepared a composite based on demineralized bone powder from mice femur combined with type I collagen and osteogenic proteins BMP-2 and BMP4 as biological factors. They were able to maintain a haematopoiesis niche, specifically blood cells for 1 week, for studying the complex tissue-level functions of bone marrow. In a bone cancer study, Marturano-Kruik *et al.*¹⁷⁴ employed calve metacarpal joints for obtaining milled bone that was later decellularized

and sterilized in ethanol to retain the mineralized trabecular structure. That structure was later added in a microfluidic chip (Fig. 5A and B) for evaluating MSCs response in a co-culture with HUVECs. Although this study focused mainly on vasculogenesis, it was found that MSCs and endothelial cells were able to attach into the trabecular space and that MSCs occupied the bone trabeculae in the existing mineral matrix and capillary-like structures within the trabecular pores (Fig. 5C and D). Also, this OOC approach demonstrated three aspects: (i) co-cultures of cancer cells with MSCs can colonize and adapt in a bone niche microenvironment; (ii) these can survive against commonly employed anticancer drugs (*i.e.*, sunitinib); and (iii) when exposed to interstitial flow, cancer cell proliferation rate was decreased 4-fold. However, a disadvantage could be that the scaffold design restricts the scalability potential due the “sponge or block” design of these scaffolds,^{124,125} which differs from the automated and systematic approaches needed for HTS.

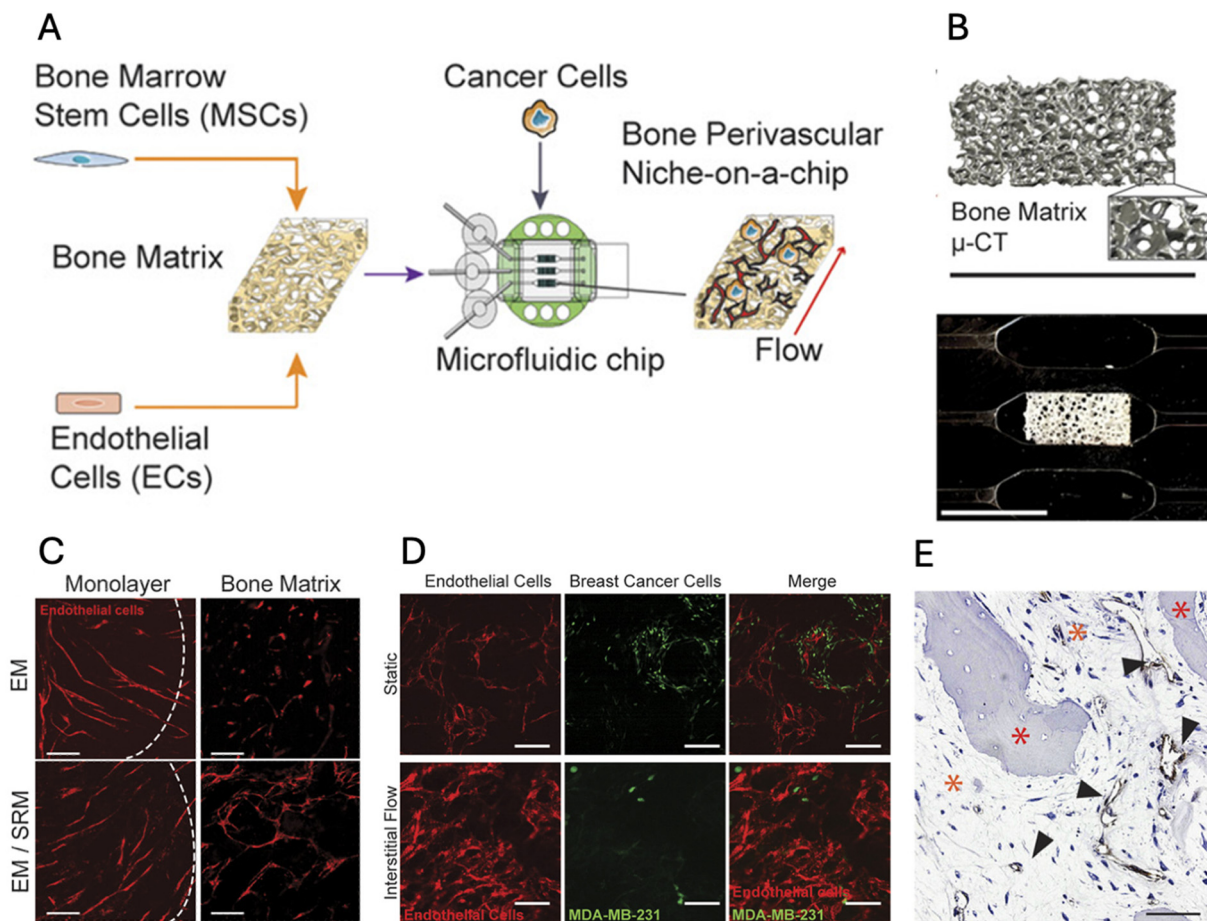


Fig. 5 Vascularized bone niche-on-a-chip model. (A) Model and study design for the generation of the bone OOC for studying breast cancer colonization. Human bone marrow derived MSCs and endothelial cells (ECs) were cultured in 3D decellularized bone matrix for biofabricating bone with a perivascular niche. (B) (Top) Chip design with scaffold consisting of decellularized bone tissue, and the image was obtained by micro-computed tomography (μ -CT) data reconstruction. (Bottom) Bone matrix in the microfluidic chip, note the transparency of the OOC device. (C) Confocal images of RFP-labelled endothelial cells that were able to form endothelial cell connections either in monolayers or in the bone matrix (scale bar: 200 μ m). (D) Live confocal images of breast cancer cells (GFP-transduced MDA-MB-231 cells) in the bone perivascular niche with interstitial flow ($\sim 3.1 \mu\text{m s}^{-1}$; bottom) vs. control (static) (scale bar: 50 μm). (E) Immunostaining of endothelial marker CD31 in the OOC showing vascular formations (arrowheads) around the trabecular pores (orange asterisk) in the bone matrix (red asterisks) (scale bar: 50 μm). Modified from Marturano-Kruik *et al.*¹⁷⁴ Publication: PNAS Publisher: Atypon publishing platform date: 23 January 2018. Copyright © 2023 National Academy of Science. All rights reserved.

Biologically-derived bone grafts have some supply difficulties that can oppose its use, such as the healthcare authority regulation, animal welfare principles of 3R and the strict aseptic handling to avoid contamination.^{15,175} Hence, bone substitutes are a good choice for being applied as the component in the scaffold formulation and they indeed have been employed in several OOC bone models.^{151,153,176} An early example is the model employed by Lee *et al.*¹⁵¹ that fabricated calcium phosphate nanoparticles of ~100 nm, 50:50 biphasic mixture of non-degradable HA and fast-degrading tricalcium phosphate for replicating new bone formation in the form of an ink containing 6% PLGA, 2% rifampicin and 2% calcium phosphate (w/w) for inkjet bioprinting into the glass slide that was later covered by the PDMS device. This early OOC approach demonstrated feasibility for efficacy testing of biomaterials and its antibiotic loading in a dynamic interaction of osteoblast and bacteria with scaling capabilities demonstrating an enhanced calcium deposition by cells (MC3T3-E1) in the matrix when calcium phosphate-containing micropatterns were present, promoting osteogenic development; this effect was not adversely influenced by the antibiotic loading of micropatterns. Another example of bone substitutes was employed by Sieber *et al.*¹⁵⁶ for a bone marrow-on-a-chip wherein HA-coated zirconium oxide-based Sponceram® scaffolds (Zellwerk GmbH) were employed with a height of 5.8 mm diameter and compared to an *in vivo* sample of bone marrow, demonstrating that haematopoietic stem and progenitor cells can be cultured for 28 days and that these progenitor cells were capable of cell colony formation, including granulocytes, erythrocytes, macrophages and megakaryocytes. Moreover, Sun *et al.*¹⁵⁸ proposed an *in vitro* model consisting of coated biphasic microbeads (20 µm diameter beads composed of 68% of HA and 32% of β-tricalcium phosphate, with collagen type I) in the culture chamber of the OOC to model the mechanotransduction of primary human osteocytes. This model was maintained with perfusion for 14 days, evidencing osteocyte interconnection between the microbeads similar to anatomical canaliculi. This replicated the *in vitro* screening of parathyroid hormone treatment and the results showed an increased RANKL matrix deposition. Also, this microfluidic perfusion culture device was able to produce cyclic compression loading by applying an artery clamp in the medium outlet, which was found to enhance cell viability with a 2.5-fold increase and decrease the production of sclerostin, a signal for new bone formation.

Some reflections emerging from these OOC studies relate specifically to the requirements of employing scaffolds as a biofabrication method for resembling the ECM inside the chips as a majority of studies have employed scaffolds in the form of hydrogels. Hydrogels, as pseudoplastic scaffold biomaterials, enable the injection of cells embedded within themselves into ready-to-use chips. Their shear-thinning behaviour allows flow and injection into chip canals. Once in place, the hydrogels can form a stable structure and maintain the attached cells while the media perfuses through the chip for a longer time. Hydrogel stabilization may happen by pure deposition if sufficient viscoelastic properties are retained, where the perfusing media flows do not disturb it, or by

possible hydrogel post-fixation utilizing cross-linking methods by means of light or enzymes.^{152,159,160,164}

Another feature to consider is the capability to observe the cells in the scaffold continuously, although some scaffolds allow direct light observation; some others such as bioceramics (*e.g.*, calcium phosphate) can hinder cell monitoring. However, this is easily tackled by terminal toxicity/viability assays, such as 3(4,5-dimethylthiazol-2-yl)-2,5-diphenyltetrazolium bromide (MTT) and other immunofluorescence assays (*e.g.*, calcein AM). There is abundant room for further progress with in-line analysis of OOC using sensors that can tackle current challenges, specifically with the employment of 3D electrodes¹⁷⁷ and other modalities that are summarized in the review from Fuchs *et al.*¹⁷⁸ Finally, we want to highlight some work examples utilising biofabrication techniques that provide reliable HTS platforms. These include

1) utilizing inkjet bioprinting with composite (biphasic CP nanoparticles dispersed in a poly(D,L-lactic-*co*-glycolic) acid matrix) hydrogel formulation;¹⁵¹

2) a non-contact dispenser robot capable of bioprinting in an easy and rapid way to operate the microfluidic channel;¹⁵⁰

3) and an automatic scanner compatible with microfluidic 96-chip plates.¹⁷²

To demonstrate a platform capable of analysing the bone remodelling cycle at the molecular level with specificity and throughput, Yvanoff *et al.*¹⁵⁰ established a bone model for studying cell-cell communication between osteocytes and osteoblasts, allowing a more realistic physiological cancer bone model than previously demonstrated. These state-of-the-art bioengineering platforms must address the challenges of scaling up for clinical trial validation while ensuring alignment with regulations and bioethical standards. Successful translation requires collaboration between academia and clinicians to advance innovative medical solutions utilizing developed bone-on-chip models.

6. Bone metastasis on chip

Bone tissue is one of the most common tumour sites for metastasis, especially for breast, prostate, and lung cancers. Among these, 65–75% of breast and prostate metastatic patients can present skeletal lesions as both represent more than 80% of all cases of metastatic bone disease.¹⁷⁹ Hence, cancer metastasis is one of the greatest challenges in cancer research, with a process being altered by multiple factors, such as stromal cells, ECM, and tumour cells themselves.¹⁷⁶ Here we present selection of articles with various OOC models that were also developed and orientated to mimic this complexity. We summarize those studies in Table 4 (ref. 174 and 180–187) that have employed some different type of MPS with cancer cells in a bone model and describe them in detail in the text below.

An early approach for studying cancer metastasis was performed by Bersini *et al.* in 2014,¹⁸⁶ one of the first OOC model using a bone matrix composed of Matrigel plus ECM deposited by osteogenic-differentiated BM-MSCs (*i.e.*, demonstrated by Alizarin Red staining of calcium deposition on



Table 4 OOC cancer-related studies with the employment of bone models OOC

Bone model	Pathology	Cell types	Mechanical stimulations	Chip material	Scaffold	Ref.
Progression and drug resistance of breast cancer cells colonizing the bone	Breast cancer metastasis	BM-MSCs (primary), breast cancer cells GFP/Luc, HUVECs/GFP	Yes, shear stress ($0.25 \mu\text{L min}^{-1}$ flow rate resulted in an average fluid velocity of $\sim 3.1 \mu\text{m s}^{-1}$ within the 3D bone matrix)	PDMS	Decellularized bone scaffold	174
Perfusible human microvascularized bone-microenvironment	Breast cancer metastasis	BM-MSCs, osteogenic cells (BM-MSCs), GFP-HUVECs	Yes, flow rate of $2 \mu\text{L min}^{-1}$, shear stress ($0.25 \text{ dyne cm}^{-2}$)	PDMS	Fibrin gel	180
Mimicking bone marrow niche and efficacy testing	Leukaemia	Eritroleukemic bone marrow derived cell lines (TF-1), hBM-MSCs	No	PDMS, glass	DBM (demineralized cancerous bone with collagen type I and IV) into $5 \times 5 \times 1$ mm chamber size	181
Bone-on-a-chip for <i>in vitro</i> studies of breast cancer bone metastasis	Breast cancer metastasis	Murine calvaria preosteoblasts (MC3T3-E1), human breast cancer cell lines, MDA-MB-231GFP	No	PDMS	Collagen and hydroxyapatite composite freeze-dried	182
Investigate the role of osteocytes in the mechanical regulation of breast cancer bone metastasis	Breast cancer metastasis	Metastatic breast cancer cells (MDA-MB-231), HUVECs, osteocyte-like cells (MLO-Y4), differentiated osteoblast (RAW246.7)	No	No	No	183
Evaluation of the relationship between ECM properties and tumour angiogenesis and metastasis	Colorectal/gastric cancer metastasis	HUVECs, human colon cancer (SW620) and human gastric cancer (MKN74)	No	PDMS	Hydroxyapatite nanocrystals ($<200 \text{ nm}$) plus fibrin composite scaffold	184
Investigate mechanical stimulation of osteocytes' influence the effect on cancer cell behaviour	Breast and prostate cancer	MLO-Y4 osteocyte-like mouse cell line, MDA-MB-231 and MCF-7, and two human prostate cancer cell lines (PC3 and LNCaP)	Yes, shear stress (oscillatory fluid flow of 0.5 Hz with an amplitude of 1.5 cm for 24 h after an initial 24 h static period post seeding)	PDMS	Rat tail collagen type I, 0.15 mg mL^{-1} ; Sigma	185
Develop of a tri-culture microfluidic 3D <i>in vitro</i> model for emulating human breast cancer cells metastasis	Breast cancer metastasis	MDA-MB-231, human bone marrow-derived MSCs (hBM-MSCs), HUVECs	No	PDMS coated with a PDL (poly-D-lysine hydrobromide; 1 mg mL^{-1} ; Sigma-Aldrich)	Matrigel™ (BD Biosciences) solution (3.0 mg mL^{-1})	186
Biomimetic multiorgan microfluidic model to study cancer metastasis	Breast cancer metastasis	MCF7 and, MDA-MB-231 breast cancer cell lines, and ACC-M salivary gland adenoid cystic carcinoma cells and HUVECs	No	PDMS layers on a glass substrate	Cultrex™ Basement Membrane Extracts	187



Matrigel). They analysed the transendothelial migration/extravasation of highly metastatic breast cancer cells (triple negative cell line) from endothelial channels into the bone matrix. This extravasation was enhanced by the presence of osteoblasts compared to the scaffold only controls, demonstrating the major roles of breast cancer cell receptor CXCR2 and the bone-secreted chemokine CXCL5 and elucidating a specific cancer cell to bone cell interaction. Although the model lacked perfusion, it was a starting point for metastasis modelling in the bone-like ECM. Next, for evaluating cancer cells in a perfused bone model, it was observed that mechanical stimulation can decrease the metastasis-induced osteolysis of breast cancer cells in an *in vitro* model developed by Marturano-Kruik *et al.* in 2018.¹⁷⁴ This group reported a 4-fold decrease in breast cancer cell growth rate in 3D cultures under perfusion. Furthermore, they also found that physiologically interstitial flow caused a decrease in the niche cancer colonization after the optimization of interstitial flow velocities and shear forces by the aid of computational fluid dynamics. This association between physical activity and cancer prognosis has been previously found in the *in vivo* experiments, and similar associations have been found with some other molecular subtypes of breast cancer.¹⁸⁸ This outcome is somehow contrary to that of Verbruggen *et al.*,¹⁸⁵ where authors evaluated the influence of mechanical loading in a way to imitate the load-bearing physical exercise and its effects on osteocytes. They

demonstrated that conditioned medium derived from osteocyte paracrine signalling usually inhibits metastatic breast cancer tumour growth (same triple negative cell line than previous study), although after mechanical loading (*i.e.*, oscillatory fluid flow), an increased invasion of breast and prostate cancer cells was observed. These two examples pave the way for OOC studies to explore critical *in vivo* factors, such as the impact of mechanical stimuli on breast cancer bone metastasis, where there are still contrasting findings.

From the perspective of resembling the bone with the ECM scaffold and how it affects cancer cells behaviour, Ahn *et al.* highlighted the importance of matrix stiffness on the cancer cellular response when OOC were employed.¹⁸⁴ They evaluated two cancer cell lines (SW620 and MKN72) that can metastasized to bone and cultured them in a series of HA/fibrin composites. A higher percentage of HA resulted in an increase in the stiffness of the scaffold, which subsequently caused an inhibitory response in cancer cell migration. This association was also observed with vascularized tumour-stromal cell spheroids, highlighting the relevance of scaffold design on the effects of bone cancer cell models. Houshmand *et al.* aimed to mimic bone marrow niche for studying acute myeloid leukaemia by applying a composite made of demineralized bone matrix cancellous allograft coated with collagen type I.¹⁸¹ This platform enabled relevant *in vitro* drug screening of cytarabine and azacitidine in erythroleukemic

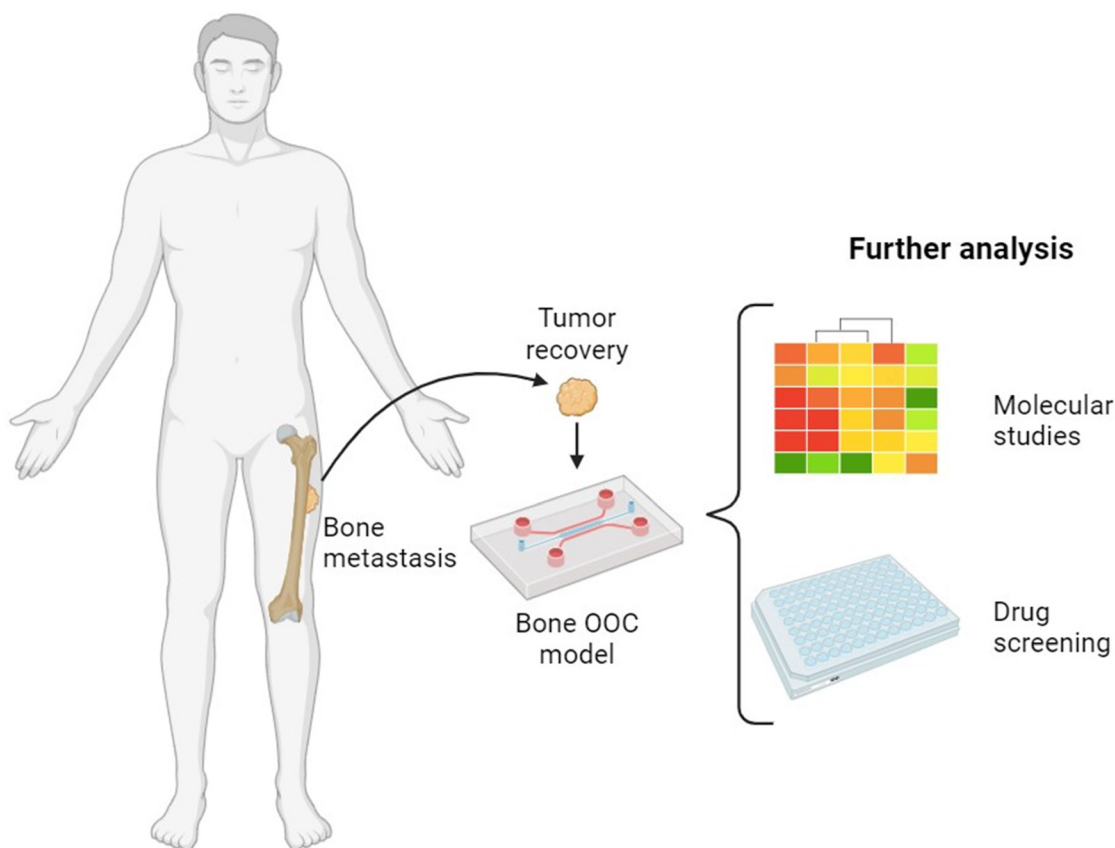


Fig. 6 Generation of bone metastasis OOC and its possible applications. Created with <https://Biorender.com>.



bone marrow-derived cell lines (TF-1), establishing a robust system for comparing the effects of different drugs and studying cancer cell behaviour. It also demonstrated that employing a 3D niche can significantly influence the drug resistance capacity of erythroleukemic cancer cells.

In summary, studies on bone cancer models demonstrate that mechanical stimulation of cancer cells in OOC devices (Fig. 6) is a critical factor,^{174,180,185} as it influences cell behavior and tissue formation. Additionally, scaffold composition and consequently its stiffness play a pivotal role in modulating cancer cell responses and their sensitivity during drug screening. However, elucidating the exact influence of different types of mechanical loadings or finding ideal components and conditions is difficult due to the different experimental methods employed across presented studies. Also, additional research is needed to better understand the complex interactions between multiple organs as physiological processes depend on regulatory pathways and hormonal feedback between organs with the endocrine system. Currently, these can be approached by generating multi-OOC platforms that can bring more accuracy and model complexity¹⁴⁸ to metastatic cells infiltration and invasion.

7. Neurovascularized bone on-a-chip

Bone is a well-vascularized and innervated tissue with a structured order of nerve and blood vessels that are arranged in a perifocal distribution of the central channel of the Haversian system (Fig. 1). Nerves are also present in the periosteum, bone marrow and Volkmann's canals.³⁸ To evaluate bone as a representative model, it is necessary to mimic the nutrient and nerve supply as an *in vivo* system to maintain the biological component until the artificial tissue accomplish a functionality ideally resembling bone tissue remodelling conditions.

The vascularization for these purposes can be broadly classified into endothelial or angiogenesis/vasculogenesis types, where the endothelial cells act mainly as a barrier attached to a membrane in an epithelial architecture.¹⁸⁹ It seems that the usual approach for bone-on-chip models is to provide 3D tubular structures as angiogenesis or vasculogenesis¹⁵⁴ that are based on the employment of chips with interstitial perfusion capabilities for stimulating bone tissue cells and HUVECs, as these allow to measure different aspects of angiogenesis processes when added to co-cultured systems.¹⁹⁰ Also, other cell types have been identified to participate in vascular morphogenesis such as stromal cells and lung fibroblasts.¹⁸⁹ An early approach to mimic vascularization was employed by Bertassoni *et al.*¹⁹⁰ that printed a template of agarose microchannels inside the crosslinked hydrogels for creating perusable microchannels that were able to promote the lining of endothelial cells.

There is an interesting baseline angiogenesis approach delivered from Babaliari *et al.*,¹⁶¹ who provided a basepoint for interstitial perfusion rate with a good description of the values for capillary mean velocity of 0.001 (m s⁻¹), diameter of 0.008 mm and flow rate of 0.003 (μL min⁻¹) imitating the vessels in

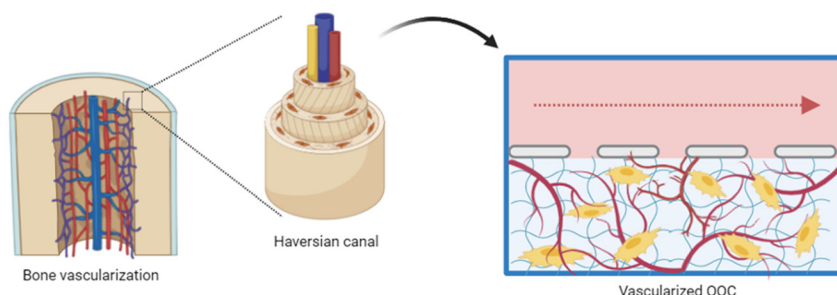
the blood circulation, with values based on previous work.^{189,190} This group produced an OOC device mimicking a perfusion flow of 30 or 50 μL min⁻¹ and shear stress of 0.3/0.03 dynes cm⁻². After establishing these flow rates, they employed a collagen type I gel for loading MC3T3-E1 osteoblast-like cells. They evidenced that mechanical stimulation produced a 4.4-fold increase in collagen production (using gelatin scaffolds in this assay), 2.4-fold increase in cell proliferation and 1.6-fold increase in ALP activity increase after 7 days of culture compared to static conditions. Jusoh *et al.*¹⁵⁴ developed a microfluidic vascularized model replicating the endothelial-induced vessel sprouting into the bone that was modelled with HA and fibrin depending on HA nanocrystal concentration (range 0.0% to 0.4%), and they found an enhanced number of sprouts and larger lumen area in 0.2% HA composite. However, the limit of this approach was the lack of use of any bone cells.

The vascularized bone model proposed by Marturano-Kruik *et al.*¹⁷⁴ was a platform enabling the evaluation of bone-metastatic breast cancer responses to an anticancer drug (3.5 μM sunitinib) using biologically-derived decellularized calve metacarpal bone as a scaffold. The biophysical stimuli of interstitial flow improved the vascularized new tissue formation as it enhanced the spreading of the capillary structure and promoted ECM deposition of perivascular markers *versus* static cultures. Also, the co-culture with human BM-MSCs supported the formation of capillary-like structures lining the vascular lumen, where a densely interconnected network of vessels running through the constructed tissue was observed (Fig. 5). Noteworthy, when breast cancer cells were exposed to interstitial flow, they demonstrated a slow-proliferative state but associated with an increased drug resistance against sunitinib, demonstrating clues about how the same cancer cells behave differently depending on the presence of perfusion *versus* static culture.

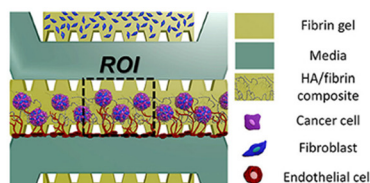
In the current tutorial review, we highlight one interesting common concept occurring within the number of papers, namely, that the formulation of composites and the component selection of the scaffold has profound implications on the cellular response and angiogenesis. This is a key point needed for consideration, particularly if long-term bone tissue engineered construct is envisaged, for example, for testing biomaterials under relevant extended bone repair time periods (up to 1 year). For this, the *in vitro* capillary network must replicate the physiological angiogenesis and vasculogenesis present in bone repair that last at least two months, replicating similar cues to that starting from hematoma formation towards scaffold-based bone formation. Based on this, an interesting approach was reported by Ahn *et al.*,¹⁸⁴ who studied how the viscoelastic properties of a scaffold based on HA and fibrin influenced the cell behaviour (Fig. 7). Depending on different HA concentrations, the storage modulus changed (without HA 0.0%/G' = 166 Pa, 0.2% HA/G' = 122 Pa and 0.4% HA/G' = 174 Pa), the authors found that HA do not significantly affect cell viability, but they found a decreased invasion response of human colon and gastric cancer cells (SW620 and MKN74) to stiffer scaffolds (Fig. 7). Even though in this model cancer cell



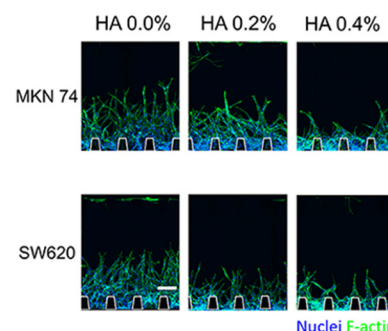
A



B



C



D

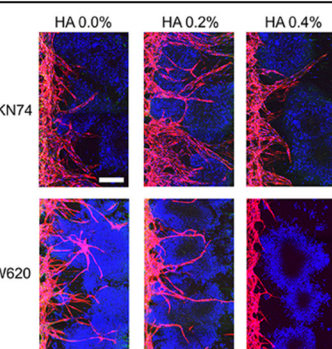


Fig. 7 Vascularized bone on chip approaches. (A) Schematic design of a bone on a chip, based on the Haversian canal vascularization. (B–D) Study design of a 3D microfluidic bone tumor microenvironment comprised of hydroxyapatite/fibrin composite. (A) Schematic of the assay to observe angiogenesis with three-dimensional tumour spheroid in the HA/fibrin composite. (C) MKN74 and SW620 cell lines in HA/fibrin composite with varying HA concentration (0.0, 0.2, and 0.4%) ($n = 5$ –9 chips per condition) (scale bar: 100 μ m). (D) MKN74 and SW620, respectively, in the HA/fibrin composite with varying HA concentration (0.0, 0.2, and 0.4%) ($n = 5$ –7 chips per condition) (scale bar: 200 μ m). Modified from Ahn *et al.*¹⁸⁴ Publication: *Frontiers in Bioengineering and Biotechnology*. Publisher: Frontiers Media S.A. © 2019, Frontiers Media S.A.

demonstrated good viability with all formulations, SW620, a colon cancer cell line had significantly decreased viability in a stiffer HA scaffold compared to the control, evidencing an anti-tumour effect of HA to this cell line, probably due the absence of mineralized components in colon tissue. Moreover, the blood vessel formation was decreased at higher HA percentage, both 0.2% and even more at 0.4% (Fig. 7), evidencing an anti-proliferation effect of HA in cell lines derived from the gastrointestinal tissue and indicating a link between the grade of mineralization and how it modulates the capillary formation when using cell lines from different tissue origins. Stiffness in colon cancer bone metastasis is relevant and important to address because colon cancer has a significant tendency to increase its stiffness in the surrounding tumour tissue when it becomes a more aggressive tumour.¹⁸⁴

The recent advances in MPS by OOC that considered modelling-vascularized tissue-engineered constructs have mostly been supported employing HUVECs. HUVECs are reported as a reliable cell source approach, leading to the versability of customizing designs with microchannels and making it possible to imitate the required vasculature. This vasculature has been shown to be affected by the employed perfusion model, making it possible to mimic a similar way to that of the complex Haversian system for structuring a bone tissue vascular network.

The innervation of bone is a complex anatomical network and plays a crucial role in bone development, remodelling,

pain sensation, and overall homeostasis. Nerve fibers are present throughout the bone and are especially concentrated in the periosteum, bone marrow, Haversian and Volkmann canals, delivering sensorial and sympathetic signals for detecting mechanical stress, influencing hematopoiesis, osteoblast and osteoclast function, nutrient exchange and mechanotransduction.¹⁹¹ Regarding this dependent interaction between bone physiology and innervation, it has been demonstrated that denervation has a pathological effect on bone development, homeostasis and repair.¹⁹² Some studies have aimed to reveal the molecular interaction between this association. Silva *et al.* utilized a PDMS-based microfluidic device¹⁶⁹ fabricated from a master mold (Fig. 8) to investigate the interaction between dorsal root ganglion neurons and MSCs. Their study demonstrated that this interaction enhances osteogenic differentiation, as evidenced by increased ALP activity and the upregulation of osteoblast-specific genes, including Runx2, Sp7, Col1a1, and bone gamma-carboxyglutamate protein, a marker associated with bone ECM mineralization.¹⁶⁹

Neto *et al.* conducted a notable study on innervation using a microfluidic-based neuro-vascularized bone chip,¹⁴⁴ which unveiled the relationship between innervation and angiogenesis in the inflammatory bone niche. This platform also served as a screening tool for studying inflammatory diseases and drug delivery systems (Fig. 9). The chip featured

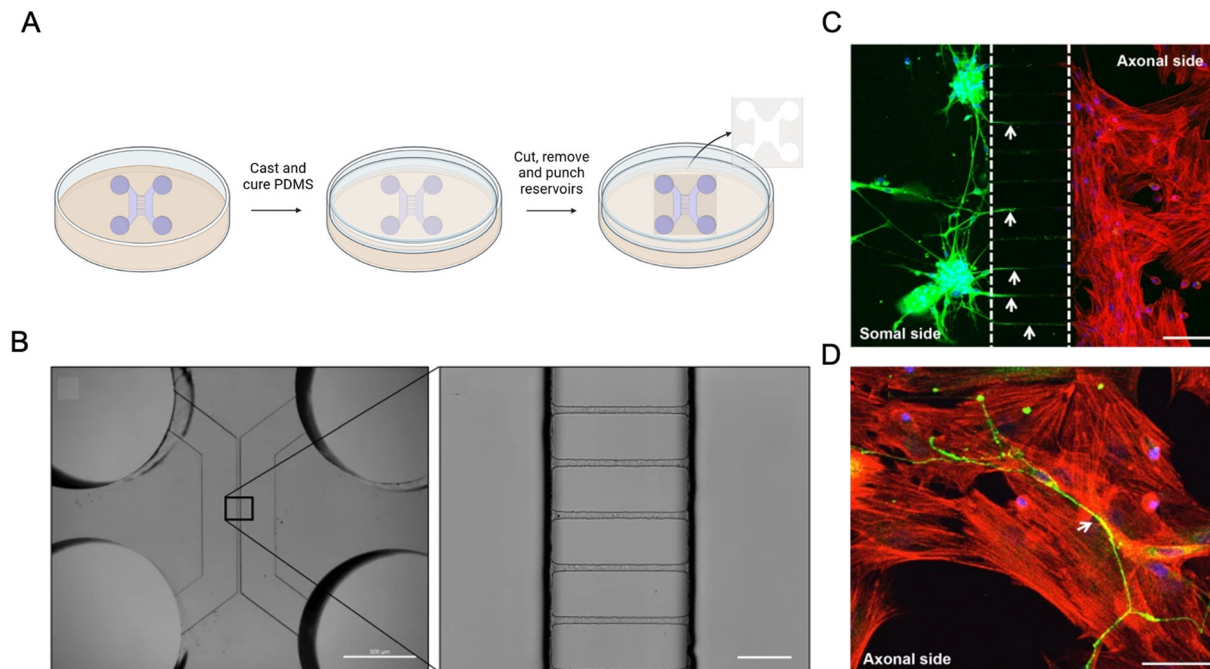


Fig. 8 Innervated bone-on-chip approach. (A) Scheme of microfluidic design, a master mold was fabricated by soft lithography and replica molding with PDMS against the master mold. Created with <https://Biorender.com>. (B) Conventional photolithography and soft lithography techniques of the microfluidic device. Scale bar = 10 μ m. (C) Sensory neurons derived from rat dorsal root ganglion and rat bone marrow MSCs cocultured in the microfluidic devices for 7 days, showing the presence of neurites (arrows) reaching MSCs by immunofluorescence. DAPI (nuclei; blue) and β -III tubulin coupled to Alexa Fluor® 488 (green). Scale bar = 100 μ m. (D) MSCs compartment showing actin filaments by Alexa Fluor® 568 phalloidin (red), nerve specific β -III tubulin and DAPI (nuclei; blue). Arrows point to neurites. Scale bar = 50 μ m. B-D are adapted from Silva *et al.*¹⁶⁹ Publication: *Cell Death & Disease*. Publisher: Springer Nature. Copyright © 2017, Springer Nature Limited.

three interconnected channels separated by semi-permeable membranes, one containing embryonic dorsal root ganglia as neurons, another with endothelial cells representing the vascular unit, and a third housing murine bone marrow cells differentiated into osteoclasts within a collagen-based scaffold. To evaluate how sensory neurons respond to an inflammatory environment, the authors employed this micropathological chip with the three cell types. Under inflammatory conditions induced by adding the pro-inflammatory cytokine IL-1 β to the osteoclast culture medium, a significant increase in axonal sprouting and extension toward the vascular zone was observed. However, this effect was mitigated by the use of ibuprofen-loaded nanoparticles, which significantly reduced axonal sprouting (Fig. 9).

In a final example, Thrivikraman *et al.*¹⁹³ introduced an intriguing approach that integrated a neuronal network within a 3D microenvironment. Though this study utilized 24-well plates instead of a microfluidic device, it successfully produced engineered bone-like tissue constructs featuring pericyte-supported blood capillaries and neuronal networks. Initially, MSC-laden collagen hydrogels were supplemented with osteopontin powder extracted from bovine milk (100 μ g mL $^{-1}$), yielding a mineral composition resembling native bone and displaying dendritic extensions morphologically similar to osteocytes. Subsequently, this mineralization protocol was replicated in a co-culture system with HUVECs and neuroblastoma cell line SH-SY5Y. This co-culture demonstrated

the early formation of vasculature and neuronal networks preceding calcification. After 18 days of culture, interconnected neuronal networks characterized by actin-rich neurites were observed, along with the expression of neuron-specific enolase and neurofilament light. Notably, the progression of mineralization did not impede vasculogenesis or neurogenesis, underscoring the compatibility of these processes within the engineered microenvironment.

8. Bone-disease personalized medicine

Over the past few decades, biomedical science has seen stunning transformation of cell culture by embracing the employment of 3D scaffolds, MPS and primary-derived cell sources. The importance of a 3D cell culture system for resembling the cell microenvironment in the matrix perspective has already been highlighted, but this powerful tool can still be enhanced by the employment of primary-derived cell from patients for studying specific features of diseases in a personalized medicine way. Studying patient-derived cells in a specific microenvironment is opening new *in vitro* assays under human-resembling designs for the measurement of specific and personalized cell behaviour, which can be applied for testing different therapeutic agents.

Primary culture is defined by the “Good Cell Culture Practice” (GCCP) as “the initial *in vitro* culture of harvested



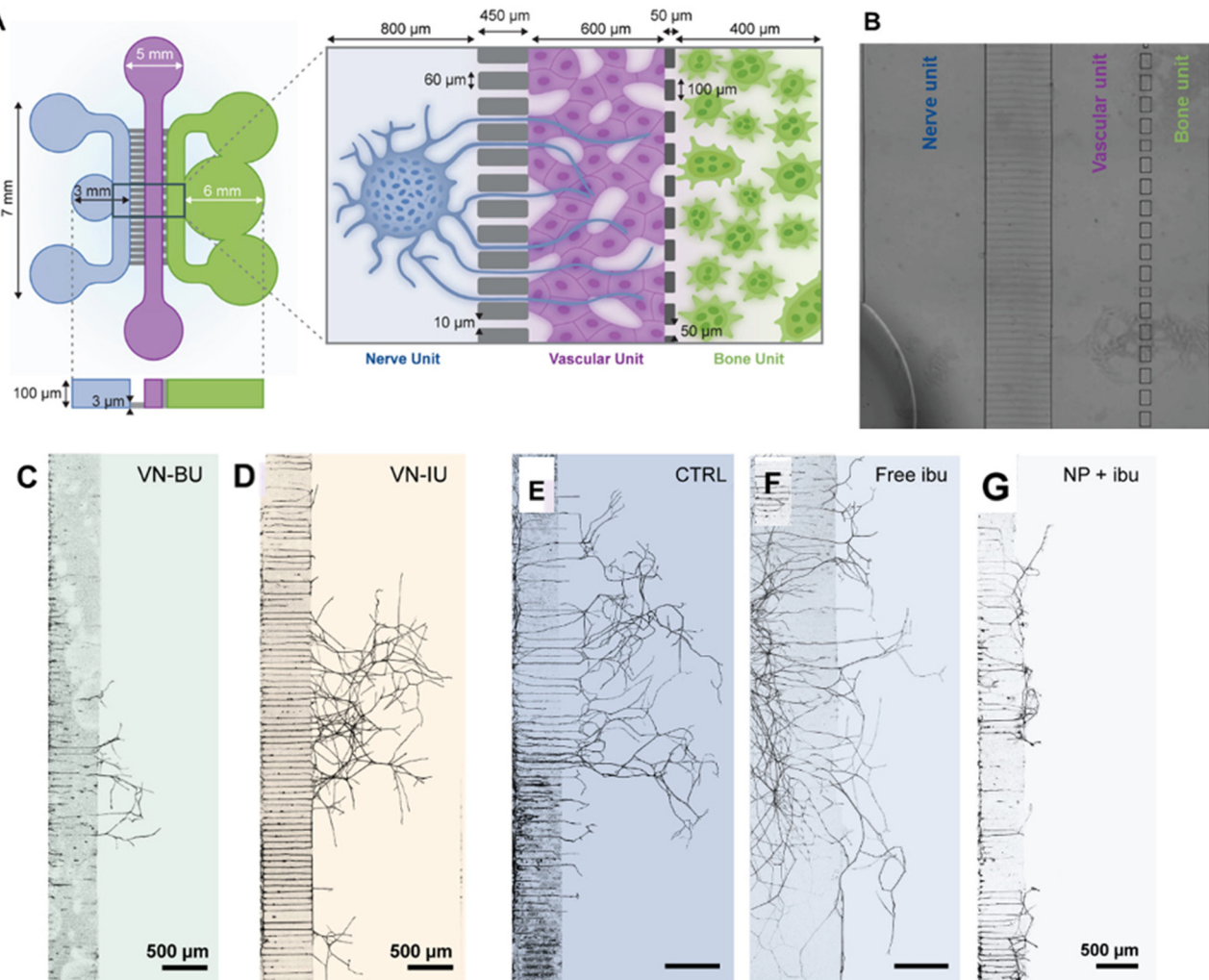


Fig. 9 Micropathological chip model of the neurovascular unit in response to an inflammatory bone condition and drug response. (A). Scheme of the bone chip with three different compartments from left to right, embryonic dorsal nerve ganglion cells, the vascular unit with HUVECs and the bone unit with osteoclasts. (B). Tile scan microscopy image of the device's microfeatures: microchannels and micropillars. Scale bar = 500 μ m. (C). Vascular network through the bone unit. (D). Inflammatory vascular network through the bone unit. (E). Axonal growth in the control condition. (F). Axonal growth image free of ibuprofen. (G). Ibuprofen-loaded PLGA NPs. NF200 in black. Scale bars = 500 μ m. Modified from Neto *et al.*¹⁴⁴ Publication: Advanced Healthcare Materials. Publisher: John Wiley and Sons Inc. Copyright © 2022.

cells and tissues taken directly from animals and humans".¹⁹⁴ Usually, these cells are derived from surgically excised tissue or as part of biopsies that are later dissociated by mechanical or enzymatic digestion, such as by collagenase type of enzymes.¹⁹⁵ Unlike the cell lines, the primary cells do not undergo immortalization manipulation with the substantial manipulation of the cell genetic material.¹⁹⁶ These cells may maintain their genetic integrity, morphology and regular cellular physiology, such as expansion and differentiation, allowing to study specific individual cellular and molecular expression under controlled microenvironment conditions that can be the first process in new *in vitro* diagnostic platforms for research and development and for establishing personalized high-throughput screening assays. For personalized medicine purposes, biopsy-derived tissue is the most common source of human cells, which, at the same time, represents several

challenges as there are important laws, regulations and bioethical principles that must be complied with. Manipulation of human-derived tissues needs ethical and biosafety authorizations as all donations have potential biological hazards that must be diminished by strict manipulation under class II biological safety cabinets with an aseptic handling technique for protecting both the personnel and the sample, and finally abiding with defined disposal protocols.¹⁹⁵ It is also mandatory that the histopathologic assessment should not be compromised, resulting in a limited quantity of tissue for diagnostic use due to the amount to be employed in research and development.¹⁹⁶ Another challenge is that cells derived from the tissue sample are a heterogeneous mixture of cell types, and it can become very difficult to select the specific cell type for studying a disease, for example, fibroblasts present in some tumours can rapidly overgrow other types of cells of interest.¹⁹⁴ For

this, several techniques have been developed for selection purposes such as mechanical disaggregation (*e.g.*, microdissection), density gradient centrifugation, cell sorting by FACS (fluorescence-activated cell sorting) or MACS (magnetic-activated cell sorting) and selective cell outgrowth by modifying the culture conditions, *e.g.*, serum-free, chemically-defined medium supplemented with specific growth factors or cytokines, allowing the proliferation of specific bone cell types.¹⁹⁴ Recently, a novel protocol for sorting different types of bone-derived and niche-derived cells has been proposed, which can narrow the specificity for studying a particular cell-specific bone disease.¹⁹⁷ Then, a second step of selection depending on the model employed can be made, such as specific cell membrane markers like homeobox protein CDX-2, to confirm intestinal origin in colon cancer metastasis in the bone.¹⁹⁸ In this case, the cells derived from biopsies and primary culture must be compatible with a type of 3D scaffolding culture systems and by combination with microfluidic systems, it can provide relevant PK/PD scenarios that can be studied.^{199,200}

Although MPS have shown to be a robust platform for *in vitro* data production, bone-personalized medicine still represents an in-development approach, as demonstrated by us among a selection of scientific literature examples. From the summary presented in this review, we draw the conclusion that the most studied is the marrow-in-a-chip approach rather than the bone cortical tissue. A myeloma research report was established by Zhang *et al.* to report a

microfluidic culture platform for studying myeloma cells from three patients,²⁰¹ demonstrating the inhibitory effect of myeloma cells on osteoblast ECM production, giving clues about the “cell adhesion-mediated drug resistance” mechanism.²⁰² A step forward in bone OOC model validation was then made by Khin *et al.*²⁰³ in this line of myeloma research with MPS and with collagen type I scaffolds to evaluate the chemosensitivity of multiple myeloma cells from 7 patients to bortezomib and melphalan. It was shown that ECM significantly increases the complexity of dose-response assays and also the heterogeneity of drug response of individual myeloma cells, bringing knowledge closer to a personalized medicine platform. Another myeloma study with MPS was employed by Pak *et al.*¹⁷⁰ with patient-derived bone marrow aspirates CD138⁺. In this case, multiple myeloma cells were sorted by CD138⁺ magnetic MACS® beads to the test chemosensitivity and chemoresistance in a co-culture approach with CD138⁻ tumour-companion mononuclear cells with the aim to resemble the tumour microenvironment (Fig. 10). Although this group did not employ a 3D ECM model, the results contributed to model validation when the data was compared with the *in vivo* outcome, constructing a future high-throughput assay for haematological malignancies that could be translated in future to bone diseases.

Nowadays, the results of personalized medicine projects that are under clinical trials with the applications of MPS are of special interest. To date, we have identified 15 clinical

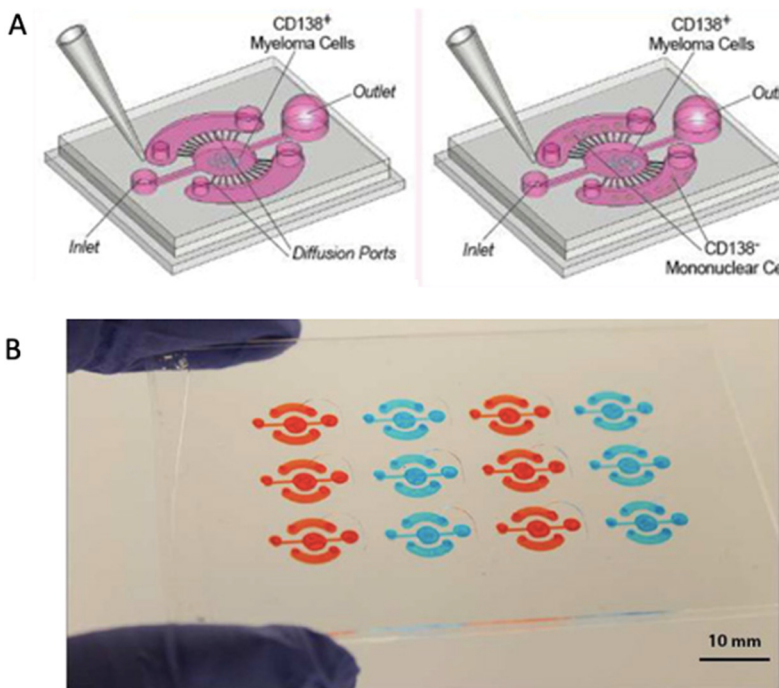


Fig. 10 Personalized bone-on-chip approach (A). Microfluidic monoculture (MicroMC) in the absence of cocultured non-tumor cell types and microfluidic-*cis*-coculture (MicroC³) incorporating patient's own CD138⁺ tumor-companion mononuclear cells. (B) A 4 × 3 array of microfluidic channels used for both MicroMC and MicroC³ is shown. (C) *Ex vivo* responses of patients' MM cells in MicroMC to bortezomib are shown. (D) *Ex vivo* responses of patients' MM cells in MicroC³ to bortezomib are shown. Modified from Pak *et al.*¹⁷⁰ Publication: Integrative Biology Publisher: Oxford University Press Date: 2015-05-22. Copyright © 2015, Oxford academic.



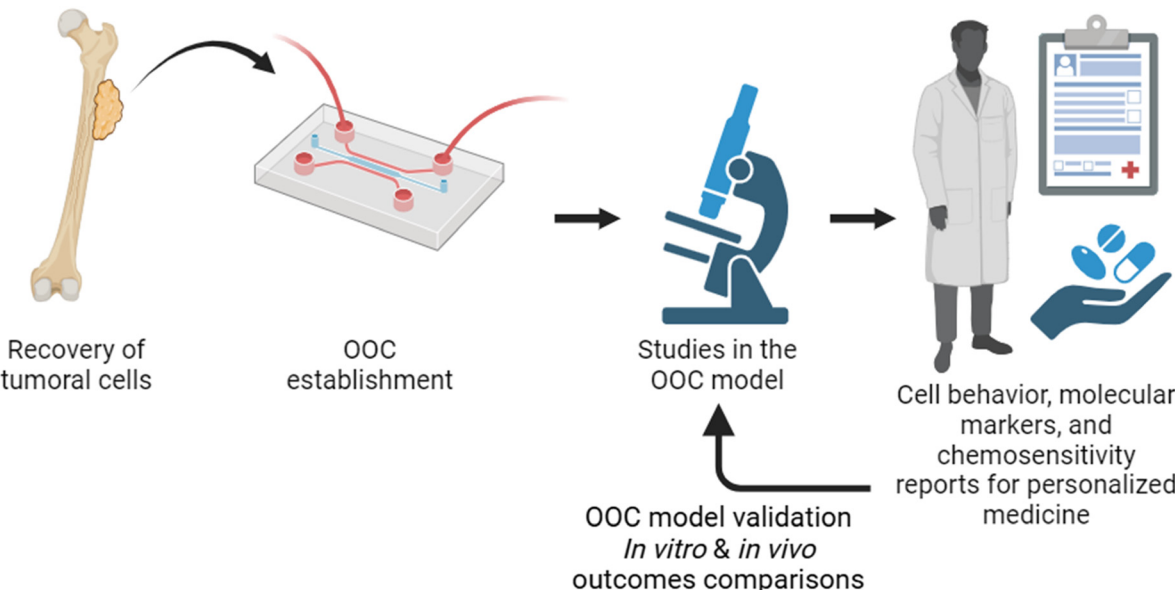


Fig. 11 Potential personalized medicine application using bone-on-chip technology. Created with <https://BioRender.com>.

trials (<https://clinicaltrials.gov>; condition/disease cancer; other terms organoid intervention/treatment personalized medicine location), among which 7 were found to be applicable to bone models. There are promising new strategies for tackling the challenges of several diseases, such as the case of the NCT06064682 trial named “An Organoid-based Functional Precision Medicine Trial in Osteosarcoma: PREMOST” employing tumor cells in Matrigel to assay multi-drug combinations, or other screening strategies. Also, there is another multicentre study (ORGANOTREAT, ID NCT05267912) for evaluating the feasibility and efficacy of organoid-based tumour in patients with histologically confirmed, unresectable, locally advanced or metastatic solid tumour. In this study, tumours derived from a biopsy are studied for patient-derived organoid generation of drug testing and producing a chemogram report with possible treatment recommendations (Fig. 11). Although these are promising approaches with use of current technologies, none of the OOC is currently registered in the <https://clinicaltrial.gov> portal for validating a new diagnostic method.

Future perspectives

Herein, we provide a summary of microfluidic approaches with important biotechnological standards for designing bone-on-chip models, aiming to tackle yet unresolved and highly prevalent bone disease models. This summary is provided with the aim to provide basis and framework towards translational human health research, features for designing platforms for HTS, precision medicine and basic science studies that can emulate human physiology, both for non-cancer and cancer related *in vitro* bone associated studies, including preclinical developments for applied

research, such as PK/PD studies for evaluating new targets,¹⁸⁰ safety and efficacy of drug candidates in cancer,^{174,181} *in vitro* diagnostic of personalized medicine, and biomaterials research & development.¹⁵¹

With the introduction of OOC, 3D cell culture can provide more physiologically relevant data as nowadays bioengineering has converged the areas of biology and mechanical engineering for establishing perfusion, emulating bioreactor properties at a small scale. Through microfluidic channels, it is now possible to bring dynamic cultures that can resemble human biomechanical stimulus, generating dynamic 3D cell culture systems that will highly decrease the quantities of materials employed and making translational-oriented research more efficient. The growing field of bone models with OOC still faces several challenges, which requires rising capabilities of inter-disciplinary collaboration for successfully operating complex platforms. These platforms will consist of lab-on-a-chip devices with multi-organ interaction and co-cultures for emulating human pathophysiology crosstalk and for determining continuous assessment of cell behaviour and viability without the requirement of ending the culture for terminal assays employing real-time monitoring of multiple cell-cell and cell-matrix interactions. Particularly, for establishing OOC for precision medicine, it is necessary to successfully implement new collaboration models between academia and clinicians, in an effort to enable the use of primary-derived cells from patients. This will help from a personalized approach point of view to better comply with healthcare regulation and bioethics exceeding several challenges of sample contamination, specificity selection of cells, in-line monitoring, and evaluating the tissue-engineered construct and 3D cell culture support in an automated and scalable approach.



To better understand bone pathophysiology and the influence of various factors, it is essential to develop systems capable of real-time data collection. This can be achieved through the integration of sensors into MPS. Sensors are compact devices designed to detect specific signals and generate continuous and reversible electronic outputs through transduction elements for computer-based condition analysis. These sensors can monitor parameters such as oxygen levels, glucose concentrations, or toxic hydrocarbons.¹⁷⁸ OOC platforms are particularly well-suited for sensor integration, benefiting from over 50 years of advancements in microelectrode technology. A notable example is the work of Bonk *et al.*,¹⁷¹ who developed a multi-sensor glass-chip incorporating a thin-film platinum sensor system. This system successfully monitored respiration, acidification, and cell adhesion within a PDMS microfluidic channel grid, enabling the characterization of pre-osteoblast (MC3T3-E1) behaviour. This innovative study, combined with ongoing sensor development, highlights new opportunities for advanced analysis in applied OOC device use. It also paves the way for integrating the real-time monitoring of patient samples into *in vitro* platforms for personalized medicine.

The implementation of HTS in OOC systems enables the collection of vast datasets, providing significant advancements in the efficacy evaluation of current drug therapies for bone diseases, with improved translation and reproducibility. A notable example is the osteocyte-targeting therapeutic screening platform developed by Lipreri *et al.*¹⁷² Using an automated scanner compatible with microfluidic 96-chip plates (Two-lane OrganoPlate® device, 9605-400-B, Mimetas BV), they evaluated the effects of teriparatide, an anti-osteoporotic drug. The study demonstrated that teriparatide significantly mitigated the cytotoxic effects of dexamethasone on osteocytes, achieving high reproducibility *in vitro*. Analysing the increasingly complex and extensive datasets generated by such platforms often surpasses the capacity of conventional statistical methods. As a result, big data analytics and artificial intelligence (AI) technologies have become indispensable. Paek *et al.*¹⁷³ showcased the groundbreaking application of AI-assisted image analysis using a deep learning platform. They compiled a database of hundreds of fluorescent images from a HTS PDMS-based bone chip to evaluate the efficacy of an anti-SOST monoclonal antibody, a therapeutic used for osteoporosis. This approach demonstrated exceptional accuracy and represented a promising platform for drug testing. Another innovative platform was developed by Xiao *et al.*²⁰⁴ integrating imaging and AI to study osteocyte morphogenesis under microfluidic shear stress using digital holographic microscopy. Although conducted on a 2D platform, their work introduced a numerical and automated method to correct imaging aberrations in holographic microscopy. By processing over 10 000 images, they significantly improved the resolution of individual cells under shear stress, enabling detailed quantitative

morphological characterization of live bone cells. These advancements highlight the transformative potential of combining HTS, AI, and advanced imaging for bone disease research and therapeutic development, particularly giving new opportunities in scaled-down OOC systems and for the implementation of quality control measures²⁰⁵ in these systems.

In the field of bone models, 3D cell culture has become widely recognized as a standard approach. Various scaffolds, both synthetic and natural, have been utilized, with collagen type I emerging as a predominant choice. This preference is likely due to its extensive history of use, particularly for coating cell culture wells.²⁰⁶ Also, we uncovered that in new OOC devices, protein-derived scaffolds based on collagen and fibrin are the most prevalent choices. However, the trend is moving towards composite biomaterials with the addition of several components, such as mineral content,^{151,154,156,158,182,184} which can provide basic bone components for the formulation in a more replicable approach with batch-to-batch reproducibility. This approach can bring together mineralized content, nanoparticles with natural^{154,182,184} or synthetic hydrogels¹⁵¹ components that can provide the necessary fluidity for dispersing cells into the OOC chambers and customized stiffness for matching the mechanobiology of the bone tissue. The use of ECM-derived components in the formulations is gaining attention with successful maintenance of complex niches demonstrated, such as bone and bone marrow.^{153,174,181} Moreover, composites with injectability capabilities can be dispensed in OOC chambers in a systematic and reproducible manner that can facilitate automation of assays for future HTS.

The cell sources of any bone model vary depending on the different scenarios of physiology and diseases processes. Currently, there are capabilities for the biofabrication of artificial tissues with specific conditions and diseases derived from patients. There are versatile scaffolds options for selecting the necessary characteristics of the pathophysiological human processes, such as customizing a specific rigidity of the ECM for a specific disease or condition. Additionally, the advances in stem cell biology can facilitate the construction of these models^{152,155,156,164,174,180} as the multipotentiality can yield tissue cell composition and enable better cell-cell interaction studies in these models. However, important challenges still remain unresolved, such as the key aspect involving the long remodelling process of bone spanning months. Such long-term cultivation strategies in MPS, up to 2–3 months, must be carefully designed to fully address the physiological process of bone remodelling. To maintain *in vitro* viable bone tissue, it is necessary to establish and provide nutrients with a functional vascularization network between the cells immersed in the mineralized tissue. Several studies have approached this with co-culture systems having vascular vessel cells. Some groups¹⁵⁴ have reported successful angiogenesis process inside the bone channel of a simple and replicable OOC



method with the formation of an angiogenic network that was influenced by the HC concentrations of the composite scaffold. Choosing the right scaffold can have deep implications on the results of these experiments and since scaffolds have very different behaviour, biocompatibility and mechanical characteristics, the right choice of components remains crucial. Moreover, an ideal scenario for studying bone and complex processes such as metastasis demands several organ-tissue interactions that increase the complexity of the model and the biofabrication demand of different cells. To successfully simulate human physiology for real 3R replacement measure and for personalized medicine, OOC must resemble the whole organism with essential biological factors such as hormonal stimulation, presence of the immune system and the microbiota, besides tissue innervation and vascularization. We hope that our tutorial review will lead to the convergence of all technologies and point towards the most prominent approaches in the field to enable future successful clinical translations from preclinical research and development and provides a new overview of guidance and key factors to achieve this.

Data availability

No primary research results, software or code have been included and no new data were generated or analysed as part of this review.

Author contributions

FVA: conceptualization, investigation, writing – original draft. JKW: conceptualization, methodology, writing – review & editing. CAVA: software, visualization. MDE: supervision, writing – review & editing. JRT: supervision, writing – review & editing, resources.

Conflicts of interest

There are no conflicts to declare.

Acknowledgements

The authors acknowledge support from the Agencia Nacional de Investigación y Desarrollo (ANID), Chile, Concurso de Fomento a la Vinculación Internacional para Instituciones de Investigación Regionales (FOVI210016), Doctorado en Biotecnología Molecular (4244002) from the Universidad de Concepción, Chile, and financial support from the AO Foundation. This work was supported by the European Union's Horizon 2020 (H2020-MSCA-IF-2019) research and innovation programme under the Marie Skłodowska-Curie grant agreement 893099 – ImmunoBioInks to J. K. W. and under the grant agreement 874790 – cmRNABone to M. D. J. K. W. would also like to acknowledge the Royal Society of Chemistry, grant (M19-6613).

References

- 1 A. Cieza, K. Causey, K. Kamenov, S. W. Hanson, S. Chatterji and T. Vos, Global estimates of the need for rehabilitation based on the Global Burden of Disease study 2019: a systematic analysis for the Global Burden of Disease Study 2019, *Lancet*, 2021, **396**(10267), 2006–2017.
- 2 A. Williams, S. J. Kamper, J. H. Wiggers, K. M. O'Brien, H. Lee and L. Wolfenden, *et al.*, Musculoskeletal conditions may increase the risk of chronic disease: a systematic review and meta-analysis of cohort studies, *BMC Med.*, 2018, **16**(1), 167.
- 3 S. N. El-Tallawy, R. Nalamasu, G. I. Salem, J. A. K. LeQuang, J. V. Pergolizzi and P. J. Christo, Management of Musculoskeletal Pain: An Update with Emphasis on Chronic Musculoskeletal Pain, *Pain Ther.*, 2021, **10**(1), 181–209.
- 4 O. Makitie and M. C. Zillikens, Early-Onset Osteoporosis, *Calcif. Tissue Int.*, 2022, **110**(5), 546–561.
- 5 X. Peng, W. Guo, T. Ren, Z. Lou, X. Lu and S. Zhang, *et al.*, Differential expression of the RANKL/RANK/OPG system is associated with bone metastasis in human non-small cell lung cancer, *PLoS One*, 2013, **8**(3), e58361.
- 6 H. L. Runolfsdottir, G. Sigurdsson, L. Franzson and O. S. Indridason, Gender comparison of factors associated with age-related differences in bone mineral density, *Arch. Osteoporos.*, 2015, **10**, 214.
- 7 X. Feng and J. M. McDonald, Disorders of bone remodeling, *Annu. Rev. Pathol.*, 2011, **6**, 121–145.
- 8 C. Wang, H. Zheng, J. W. He, H. Zhang, H. Yue and W. W. Hu, *et al.*, Genetic polymorphisms in the mevalonate pathway affect the therapeutic response to alendronate treatment in postmenopausal Chinese women with low bone mineral density, *Pharmacogenomics J.*, 2015, **15**(2), 158–164.
- 9 R. S. Day, What Tumor Dynamics Modeling Can Teach us About Exploiting the Stem-Cell View for Better Cancer Treatment, *Cancer Inf.*, 2015, **14**(Suppl 2), 25–36.
- 10 M. Schlander, K. Hernandez-Villafuerte, C. Y. Cheng, J. Mestre-Ferrandiz and M. Baumann, How Much Does It Cost to Research and Develop a New Drug? A Systematic Review and Assessment, *Pharmacoeconomics*, 2021, **39**(11), 1243–1269.
- 11 D. Guinn, E. E. Wilhelm and I. Shoulson, Reasons for Premature Conclusion of Late Phase Clinical Trials: An Analysis of ClinicalTrials.gov Registered Phase III Trials, *Ther. Innov. Regul. Sci.*, 2020, **54**(1), 232–239.
- 12 J. Arrowsmith and P. Miller, Trial watch: phase II and phase III attrition rates 2011–2012, *Nat. Rev. Drug Discovery*, 2013, **12**(8), 569.
- 13 K. H. Nam, A. S. Smith, S. Lone, S. Kwon and D. H. Kim, Biomimetic 3D Tissue Models for Advanced High-Throughput Drug Screening, *J. Lab. Autom.*, 2015, **20**(3), 201–215.
- 14 E. A. Patterson, M. P. Whelan and A. P. Worth, The role of validation in establishing the scientific credibility of



predictive toxicology approaches intended for regulatory application, *Comput. Toxicol.*, 2021, **17**, 100144.

15 A. Knight, Systematic reviews of animal experiments demonstrate poor human clinical and toxicological utility, *ATLA, Altern. Lab. Anim.*, 2007, **35**(6), 641–659.

16 N. T. Doncheva, O. Palasca, R. Yarani, T. Litman, C. Anthan and M. A. M. Groenen, *et al.*, Human pathways in animal models: possibilities and limitations, *Nucleic Acids Res.*, 2021, **49**(4), 1859–1871.

17 L. P. Hatt, A. R. Armiento, K. Mys, K. Thompson, M. Hildebrand and D. Nehrbass, *et al.*, Standard in vitro evaluations of engineered bone substitutes are not sufficient to predict in vivo preclinical model outcomes, *Acta Biomater.*, 2023, **156**, 177–189.

18 P. Horvath, N. Aulner, M. Bickle, A. M. Davies, E. D. Nery and D. Ebner, *et al.*, Screening out irrelevant cell-based models of disease, *Nat. Rev. Drug Discovery*, 2016, **15**(11), 751–769.

19 B. Clarke, Normal bone anatomy and physiology, *Clin. J. Am. Soc. Nephrol.*, 2008, **3**(Suppl 3), S131–S139.

20 J. D. Currey, The design of mineralised hard tissues for their mechanical functions, *J. Exp. Biol.*, 1999, **202**(Pt 23), 3285–3294.

21 W. E. B. M. Launey and R. O. Ritchie, On the mechanistic origins of toughness in bone, *Annu. Rev. Mater. Res.*, 2010, **40**, 25–53.

22 A. Pacureanu, M. Langer, E. Boller, P. Tafforeau and F. Peyrin, Nanoscale imaging of the bone cell network with synchrotron X-ray tomography: optimization of acquisition setup, *Med. Phys.*, 2012, **39**(4), 2229–2238.

23 X. Sun, X. Jiao, X. Yang, J. Ma, T. Wang and W. Jin, *et al.*, 3D bioprinting of osteon-mimetic scaffolds with hierarchical microchannels for vascularized bone tissue regeneration, *Biofabrication*, 2022, **14**(3), 035008.

24 D. M. E. T. Cullinane, Biomechanics of bone, in *Principles of bone biology*, ed. J. P. R. L. Bilezikian and G. A. Rodan, Academic Press, San Diego, 2002, pp. 17–32.

25 F. Linde and I. Hvid, The effect of constraint on the mechanical behaviour of trabecular bone specimens, *J. Biomech.*, 1989, **22**(5), 485–490.

26 A. Rohlmann, H. Zilch, G. Bergmann and R. Kolbel, Material properties of femoral cancellous bone in axial loading. Part I: Time independent properties, *Arch. Orthop. Trauma Surg.*, 1980, **97**(2), 95–102.

27 H. M. Frost, Bone's mechanostat: a 2003 update, *Anat. Rec., Part A*, 2003, **275**(2), 1081–1101.

28 P. E. Boulais and P. S. Frenette, Making sense of hematopoietic stem cell niches, *Blood*, 2015, **125**(17), 2621–2629.

29 S. Pfeiffer, Variability in osteon size in recent human populations, *Am. J. Phys. Anthropol.*, 1998, **106**(2), 219–227.

30 V. J. N. S. Cvetkovic, J. S. Rajkovic, A. L. J. Zabar, P. J. Vasiljevic and L. J. B. Djordjevic, *et al.*, A comparison of the microarchitecture of lower limb long bones between some animal models and humans: A review, *Vet. Med.*, 2013, **58**(7), 339–351.

31 W. J. Landis, K. J. Hodgens, J. Arena, M. J. Song and B. F. McEwen, Structural relations between collagen and mineral in bone as determined by high voltage electron microscopic tomography, *Microsc. Res. Tech.*, 1996, **33**(2), 192–202.

32 W. J. Landis, K. J. Hodgens, M. J. Song, J. Arena, S. Kiyonaga and M. Marko, *et al.*, Mineralization of collagen may occur on fibril surfaces: evidence from conventional and high-voltage electron microscopy and three-dimensional imaging, *J. Struct. Biol.*, 1996, **117**(1), 24–35.

33 J. Y. Rho, L. Kuhn-Spearing and P. Ziopoulos, Mechanical properties and the hierarchical structure of bone, *Med. Eng. Phys.*, 1998, **20**(2), 92–102.

34 P. G. H. Fratzl, E. P. Paschalis and P. Roschger, Structure and mechanical quality of the collagen-mineral nanocomposite in bone, *J. Mater. Chem.*, 2004, **14**, 2115–2123.

35 D. Taylor, Failure Processes in Hard and Soft Tissues, in *Comprehensive Structural Integrity*, ed. F. S. W. Aliabadi, Elsevier, Oxford, UK, 1st edn, 2003, vol. 9, pp. 35–95.

36 D. Taylor, J. G. Hazenberg and T. C. Lee, Living with cracks: damage and repair in human bone, *Nat. Mater.*, 2007, **6**(4), 263–268.

37 M. O. Agerbaek, E. F. Eriksen, J. Kragstrup, L. Mosekilde and F. Melsen, A reconstruction of the remodelling cycle in normal human cortical iliac bone, *Bone Miner.*, 1991, **12**(2), 101–112.

38 M. H. P. W. Ross, *Histology: A Text and Atlas*, Lippincott Williams & Wilkins, Philadelphia, 2010.

39 R. R. Rao and J. P. Stegemann, Cell-based approaches to the engineering of vascularized bone tissue, *Cyotherapy*, 2013, **15**(11), 1309–1322.

40 S. Theoleyre, Y. Wittrant, S. K. Tat, Y. Fortun, F. Redini and D. Heymann, The molecular triad OPG/RANK/RANKL: involvement in the orchestration of pathophysiological bone remodeling, *Cytokine Growth Factor Rev.*, 2004, **15**(6), 457–475.

41 J. Klein-Nulend, R. G. Bacabac and M. G. Mullender, Mechanobiology of bone tissue, *Pathol. Biol.*, 2005, **53**(10), 576–580.

42 T. Ackbarow, D. Sen, C. Thaulow and M. J. Buehler, Alpha-helical protein networks are self-protective and flaw-tolerant, *PLoS One*, 2009, **4**(6), e6015.

43 Z. Qin, L. Kreplak and M. J. Buehler, Hierarchical structure controls nanomechanical properties of vimentin intermediate filaments, *PLoS One*, 2009, **4**(10), e7294.

44 P. Fratzl, Biomimetic materials research: what can we really learn from nature's structural materials?, *J. R. Soc., Interface*, 2007, **4**(15), 637–642.

45 R. L. Hunter and A. M. Agnew, Intraskelatal variation in human cortical osteocyte lacunar density: Implications for bone quality assessment, *Bone Rep.*, 2016, **5**, 252–261.

46 F. L. Bach-Gansmo, A. Bruel, M. V. Jensen, E. N. Ebbesen, H. Birkedal and J. S. Thomsen, Osteocyte lacunar properties and cortical microstructure in human iliac crest as a function of age and sex, *Bone*, 2016, **91**, 11–19.

47 F. Marcu, F. Bogdan, G. Mutiu and L. Lazar, The histopathological study of osteoporosis, *Rom. J. Morphol. Embryol.*, 2011, **52**(1 Suppl), 321–325.



48 I. Akkawi and H. Zmerly, Osteoporosis: Current Concepts, *Joints*, 2018, **6**(2), 122–127.

49 B. M. Misof, S. Gamsjaeger, A. Cohen, B. Hofstetter, P. Roschger and E. Stein, *et al.*, Bone material properties in premenopausal women with idiopathic osteoporosis, *J. Bone Miner. Res.*, 2012, **27**(12), 2551–2561.

50 G. E. Sroga and D. Vashishth, Phosphorylation of Extracellular Bone Matrix Proteins and Its Contribution to Bone Fragility, *J. Bone Miner. Res.*, 2018, **33**(12), 2214–2229.

51 L. Ravazzano, G. Colaianni, A. Tarakanova, Y. B. Xiao, M. Grano and F. Libonati, Multiscale and multidisciplinary analysis of aging processes in bone, *npj Aging*, 2024, **10**(1), 28.

52 J. C. Marini, A. Forlino, H. P. Bachinger, N. J. Bishop, P. H. Byers and A. Paepe, *et al.*, Osteogenesis imperfecta, *Nat. Rev. Dis. Primers*, 2017, **3**, 17052.

53 N. Bishop, Bone Material Properties in Osteogenesis Imperfecta, *J. Bone Miner. Res.*, 2016, **31**(4), 699–708.

54 L. Imbert, J. C. Auregan, K. Pernelle and T. Hoc, Mechanical and mineral properties of osteogenesis imperfecta human bones at the tissue level, *Bone*, 2014, **65**, 18–24.

55 M. Ehnman and O. Larsson, Microenvironmental Targets in Sarcoma, *Front. Oncol.*, 2015, **5**, 248.

56 J. Cui, D. Dean, F. J. Hornicek, Z. Chen and Z. Duan, The role of extracellular matrix in osteosarcoma progression and metastasis, *J. Exp. Clin. Cancer Res.*, 2020, **39**(1), 178.

57 Y. Zheng, G. Wang, R. Chen, Y. Hua and Z. Cai, Mesenchymal stem cells in the osteosarcoma microenvironment: their biological properties, influence on tumor growth, and therapeutic implications, *Stem Cell Res. Ther.*, 2018, **9**(1), 22.

58 Z. Shoaib, T. M. Fan and J. M. K. Irudayaraj, Osteosarcoma mechanobiology and therapeutic targets, *Br. J. Pharmacol.*, 2022, **179**(2), 201–217.

59 A. Sekita, A. Matsugaki and T. Nakano, Disruption of collagen/apatite alignment impairs bone mechanical function in osteoblastic metastasis induced by prostate cancer, *Bone*, 2017, **97**, 83–93.

60 A. M. A. Sekita and T. Nakano, Disruption of collagen matrix alignment in osteolytic bone metastasis induced by breast cancer, *Mater. Trans.*, 2016, **57**(12), 2077–2082.

61 A. Flobak, S. S. Skanland, E. Hovig, K. Tasken and H. G. Russnes, Functional precision cancer medicine: drug sensitivity screening enabled by cell culture models, *Trends Pharmacol. Sci.*, 2022, **43**(11), 973–985.

62 X. Guan and S. Huang, Advances in the application of 3D tumor models in precision oncology and drug screening, *Front. Bioeng. Biotechnol.*, 2022, **10**, 1021966.

63 R. L. Walker, F. J. Hornicek and Z. Duan, Advances in the development of chordoma models for drug discovery and precision medicine, *Biochim. Biophys. Acta, Rev. Cancer*, 2022, **1877**(6), 188812.

64 M. J. Bissell, H. G. Hall and G. Parry, How does the extracellular matrix direct gene expression?, *J. Theor. Biol.*, 1982, **99**(1), 31–68.

65 F. Pampaloni, E. G. Reynaud and E. H. Stelzer, The third dimension bridges the gap between cell culture and live tissue, *Nat. Rev. Mol. Cell Biol.*, 2007, **8**(10), 839–845.

66 M. Ravi, V. Paramesh, S. R. Kaviya, E. Anuradha and F. D. Solomon, 3D cell culture systems: advantages and applications, *J. Cell. Physiol.*, 2015, **230**(1), 16–26.

67 R. Edmondson, J. J. Broglie, A. F. Adcock and L. Yang, Three-dimensional cell culture systems and their applications in drug discovery and cell-based biosensors, *Assay Drug Dev. Technol.*, 2014, **12**(4), 207–218.

68 S. I. Montanez-Sauri, D. J. Beebe and K. E. Sung, Microscale screening systems for 3D cellular microenvironments: platforms, advances, and challenges, *Cell. Mol. Life Sci.*, 2015, **72**(2), 237–249.

69 S. Sittampalam, R. Eglen, S. Ferguson, J. T. Maynes, K. Olden and L. Schrader, *et al.*, Three-Dimensional Cell Culture Assays: Are They More Predictive of In Vivo Efficacy than 2D Monolayer Cell-Based Assays?, *Assay Drug Dev. Technol.*, 2015, **13**(5), 254–261.

70 S. L. Ryan, A. M. Baird, G. Vaz, A. J. Urquhart, M. Senge and D. J. Richard, *et al.*, Drug Discovery Approaches Utilizing Three-Dimensional Cell Culture, *Assay Drug Dev. Technol.*, 2016, **14**(1), 19–28.

71 I. Yuste, F. C. Luciano, E. Gonzalez-Burgos, A. Lalatsa and D. R. Serrano, Mimicking bone microenvironment: 2D and 3D in vitro models of human osteoblasts, *Pharmacol. Res.*, 2021, **169**, 105626.

72 B. Al-Kaabneh, B. Frisch and O. S. Aljitalwi, The Potential Role of 3D In Vitro Acute Myeloid Leukemia Culture Models in Understanding Drug Resistance in Leukemia Stem Cells, *Cancers*, 2022, **14**(21), 5252.

73 J. Ceccato, M. Piazza, M. Pizzi, S. Manni, F. Piazza and I. Caputo, *et al.*, A bone-based 3D scaffold as an in-vitro model of microenvironment-DLBCL lymphoma cell interaction, *Front. Oncol.*, 2022, **12**, 947823.

74 E. Knight and S. Przyborski, Advances in 3D cell culture technologies enabling tissue-like structures to be created in vitro, *J. Anat.*, 2015, **227**(6), 746–756.

75 G. Liu, M. Pastakia, M. B. Fenn and V. Kishore, Saos-2 cell-mediated mineralization on collagen gels: Effect of densification and bioglass incorporation, *J. Biomed. Mater. Res., Part A*, 2016, **104**(5), 1121–1134.

76 D. C. Chow, L. A. Wenning, W. M. Miller and E. T. Papoutsakis, Modeling pO(2) distributions in the bone marrow hematopoietic compartment. II. Modified Kroghian models, *Biophys. J.*, 2001, **81**(2), 685–696.

77 W. Metzger, L. Schimmelpfennig, B. Schwab, D. Sossong, N. Dorst and M. Bubel, *et al.*, Expansion and differentiation of human primary osteoblasts in two- and three-dimensional culture, *Biotech. Histochem.*, 2013, **88**(2), 86–102.

78 J. Sasaki, T. Matsumoto, H. Egusa, M. Matsusaki, A. Nishiguchi and T. Nakano, *et al.*, In vitro reproduction of endochondral ossification using a 3D mesenchymal stem cell construct, *Integr. Biol.*, 2012, **4**(10), 1207–1214.

79 J. Wang, Y. Ye, H. Tian, S. Yang, X. Jin and W. Tong, *et al.*, In vitro osteogenesis of human adipose-derived stem cells



by coculture with human umbilical vein endothelial cells, *Biochem. Biophys. Res. Commun.*, 2011, **412**(1), 143–149.

80 M. S. Laranjeira, M. H. Fernandes and F. J. Monteiro, Reciprocal induction of human dermal microvascular endothelial cells and human mesenchymal stem cells: time-dependent profile in a co-culture system, *Cell Proliferation*, 2012, **45**(4), 320–334.

81 D. Steiner, F. Lampert, G. B. Stark and G. Finkenzeller, Effects of endothelial cells on proliferation and survival of human mesenchymal stem cells and primary osteoblasts, *J. Orthop. Res.*, 2012, **30**(10), 1682–1689.

82 Y. Xue, Z. Xing, S. Helle, K. Arvidson and K. Mustafa, Endothelial cells influence the osteogenic potential of bone marrow stromal cells, *Biomed. Eng. Online*, 2009, **8**, 34.

83 M. T. Kozlowski, C. J. Crook and H. T. Ku, Towards organoid culture without Matrigel, *Commun. Biol.*, 2021, **4**(1), 1387.

84 I. Krupa, N. J. Treacy, S. Clerkin, J. L. Davis, A. F. Miller and A. Saiani, *et al.*, Protocol for the Growth and Maturation of hiPSC-Derived Kidney Organoids using Mechanically Defined Hydrogels, *Curr. Protoc.*, 2024, **4**(7), e1096.

85 Z. Deng, H. Wang, J. Liu, Y. Deng and N. Zhang, Comprehensive understanding of anchorage-independent survival and its implication in cancer metastasis, *Cell Death Dis.*, 2021, **12**(7), 629.

86 S. Sieh, A. V. Taubenberger, S. C. Rizzi, M. Sadowski, M. L. Lehman and A. Rockstroh, *et al.*, Phenotypic characterization of prostate cancer LNCaP cells cultured within a bioengineered microenvironment, *PLoS One*, 2012, **7**(9), e40217.

87 T. Xu, K. W. Binder, M. Z. Albanna, D. Dice, W. Zhao and J. J. Yoo, *et al.*, Hybrid printing of mechanically and biologically improved constructs for cartilage tissue engineering applications, *Biofabrication*, 2013, **5**(1), 015001.

88 J. Jeon, M. S. Lee and H. S. Yang, Differentiated osteoblasts derived decellularized extracellular matrix to promote osteogenic differentiation, *Biomater. Res.*, 2018, **22**, 4.

89 S. Phothichailert, N. Nowwarote, B. P. J. Fournier, V. Trachoo, S. Roytrakul and W. Namangkalakul, *et al.*, Effects of decellularized extracellular matrix derived from Jagged1-treated human dental pulp stem cells on biological responses of stem cells isolated from apical papilla, *Front. Cell Dev. Biol.*, 2022, **10**, 948812.

90 C. Gao, L. Fu, Y. Yu, X. Zhang, X. Yang and Q. Cai, Strategy of a cell-derived extracellular matrix for the construction of an osteochondral interlayer, *Biomater. Sci.*, 2022, **10**(22), 6472–6485.

91 S. Lee, D. N. Burner, T. R. Mendoza, M. T. Muldong, C. Arreola and C. N. Wu, *et al.*, Establishment and Analysis of Three-Dimensional (3D) Organoids Derived from Patient Prostate Cancer Bone Metastasis Specimens and their Xenografts, *J. Visualized Exp.*, 2020(156), e60367.

92 F. E. Froeling, J. F. Marshall and H. M. Kocher, Pancreatic cancer organotypic cultures, *J. Biotechnol.*, 2010, **148**(1), 16–23.

93 P. Timpson, E. J. McGhee, Z. Erami, M. Nobis, J. A. Quinn and M. Edward, *et al.*, Organotypic collagen I assay: a malleable platform to assess cell behaviour in a 3-dimensional context, *J. Visualized Exp.*, 2011, **56**, e3089.

94 J. Havel, H. Link, M. Hofinger, E. Franco-Lara and D. Weuster-Botz, Comparison of genetic algorithms for experimental multi-objective optimization on the example of medium design for cyanobacteria, *Biotechnol. J.*, 2006, **1**(5), 549–555.

95 R. Shaw, M. Fitzek, E. Mouchet, G. Walker and P. Jarvis, Overcoming obstacles in the implementation of factorial design for assay optimization, *Assay Drug Dev. Technol.*, 2015, **13**(2), 88–93.

96 F. Pampaloni, U. Berge, A. Marmaras, P. Horvath, R. Kroschewski and E. H. Stelzer, Tissue-culture light sheet fluorescence microscopy (TC-LSFM) allows long-term imaging of three-dimensional cell cultures under controlled conditions, *Integr. Biol.*, 2014, **6**(10), 988–998.

97 M. Castilho, M. de Ruijter, S. Beirne, C. C. Villette, K. Ito and G. G. Wallace, *et al.*, Multitechnology Biofabrication: A New Approach for the Manufacturing of Functional Tissue Structures?, *Trends Biotechnol.*, 2020, **38**(12), 1316–1328.

98 J. A. B. S. Planell, D. Lacroix and A. Merolli, *Bone Repair Biomaterials*, Woodhead Publishing, Sawston, UK, 2009.

99 G. N. Bancroft, V. I. Sikavitsas, J. van den Dolder, T. L. Sheffield, C. G. Ambrose and J. A. Jansen, *et al.*, Fluid flow increases mineralized matrix deposition in 3D perfusion culture of marrow stromal osteoblasts in a dose-dependent manner, *Proc. Natl. Acad. Sci. U. S. A.*, 2002, **99**(20), 12600–12605.

100 T. Albrektsson and C. Johansson, Osteoinduction, osteoconduction and osseointegration, *Eur. Spine J.*, 2001, **10**(Suppl 2), S96–S101.

101 D. Mitra, J. Whitehead, O. W. Yasui and J. K. Leach, Bioreactor culture duration of engineered constructs influences bone formation by mesenchymal stem cells, *Biomaterials*, 2017, **146**, 29–39.

102 S. L. L. X. Wu, K. W. K. Yeung, C. S. Liu and X. J. Yang, Biomimetic porous scaffolds for bone tissue engineering, *Mater. Sci. Eng., R*, 2014, **80**, 1–36.

103 J. D. Humphrey, E. R. Dufresne and M. A. Schwartz, Mechanotransduction and extracellular matrix homeostasis, *Nat. Rev. Mol. Cell Biol.*, 2014, **15**(12), 802–812.

104 J. Swift, I. L. Ivanovska, A. Buxboim, T. Harada, P. C. Dingal and J. Pinter, *et al.*, Nuclear lamin-A scales with tissue stiffness and enhances matrix-directed differentiation, *Science*, 2013, **341**(6149), 1240104.

105 C. Ai, L. Liu and J. C. Goh, Pore size modulates in vitro osteogenesis of bone marrow mesenchymal stem cells in fibronectin/gelatin coated silk fibroin scaffolds, *Mater. Sci. Eng., C*, 2021, **124**, 112088.

106 H. J. Sung, C. Meredith, C. Johnson and Z. S. Galis, The effect of scaffold degradation rate on three-dimensional cell growth and angiogenesis, *Biomaterials*, 2004, **25**(26), 5735–5742.



107 F. Stojeeski, A. Buetti-Dinh, M. J. Stoddart, A. Danani, E. Della Bella and G. Grasso, Influence of dexamethasone on the interaction between glucocorticoid receptor and SOX9: A molecular dynamics study, *J. Mol. Graphics Modell.*, 2023, **125**, 108587.

108 D. H. L. Van der Heide, E. Della Bella, A. Hangartner, W. A. Lackington, H. Yuan, F. De Groot-Barrère, M. J. Stoddart and M. D'Este, Characterization and biological evaluation of 3D printed composite ink consisting of collagen, hyaluronic acid and calcium phosphate for bone regeneration, *Carbohydr. Polym. Technol. Appl.*, 2024, **7**, 100518.

109 A. R. H. L. Armiento, G. Sanchez Rosenberg, K. Thompson and M. J. Stoddart, Functional Biomaterials for Bone Regeneration: A Lesson in Complex Biology, *Adv. Funct. Mater.*, 2020, **30**, 1909874.

110 C. M. Murphy, M. G. Haugh and F. J. O'Brien, The effect of mean pore size on cell attachment, proliferation and migration in collagen-glycosaminoglycan scaffolds for bone tissue engineering, *Biomaterials*, 2010, **31**(3), 461–466.

111 T. M. Keaveny, E. F. Morgan, G. L. Niebur and O. C. Yeh, Biomechanics of trabecular bone, *Annu. Rev. Biomed. Eng.*, 2001, **3**, 307–333.

112 D. M. Cooper, C. E. Kawalilak, K. Harrison, B. D. Johnston and J. D. Johnston, Cortical Bone Porosity: What Is It, Why Is It Important, and How Can We Detect It?, *Curr. Osteoporos. Rep.*, 2016, **14**(5), 187–198.

113 D. M. Cooper, J. R. Matyas, M. A. Katzenberg and B. Hallgrímsson, Comparison of microcomputed tomographic and microradiographic measurements of cortical bone porosity, *Calcif. Tissue Int.*, 2004, **74**(5), 437–447.

114 C. M. Murphy, G. P. Duffy, A. Schindeler and F. J. O'Brien, Effect of collagen-glycosaminoglycan scaffold pore size on matrix mineralization and cellular behavior in different cell types, *J. Biomed. Mater. Res., Part A*, 2016, **104**(1), 291–304.

115 S. F. El-Amin, M. D. Kofron, M. A. Attawia, H. H. Lu, R. S. Tuan and C. T. Laurencin, Molecular regulation of osteoblasts for tissue engineered bone repair, *Clin. Orthop. Relat. Res.*, 2004, **427**, 220–225.

116 M. P. Lutolf, Integration column: artificial ECM: expanding the cell biology toolbox in 3D, *Integr. Biol.*, 2009, **1**(3), 235–241.

117 E. Ruoslahti, RGD and other recognition sequences for integrins, *Annu. Rev. Cell Dev. Biol.*, 1996, **12**, 697–715.

118 R. K. Sinha and R. S. Tuan, Regulation of human osteoblast integrin expression by orthopedic implant materials, *Bone*, 1996, **18**(5), 451–457.

119 Y. L. Wang, S. P. Lin, S. R. Nelli, F. K. Zhan, H. Cheng and T. S. Lai, *et al.*, Self-Assembled Peptide-Based Hydrogels as Scaffolds for Proliferation and Multi-Differentiation of Mesenchymal Stem Cells, *Macromol. Biosci.*, 2017, **17**(4), 1600192.

120 M. J. Dalby, N. Gadegaard, R. Tare, A. Andar, M. O. Riehle and P. Herzyk, *et al.*, The control of human mesenchymal cell differentiation using nanoscale symmetry and disorder, *Nat. Mater.*, 2007, **6**(12), 997–1003.

121 A. Basillaïs, S. Bensamoun, C. Chappard, B. Brunet-Imbault, G. Lemineur and B. Ilharreborde, *et al.*, Three-dimensional characterization of cortical bone microstructure by microcomputed tomography: validation with ultrasonic and microscopic measurements, *J. Orthop. Sci.*, 2007, **12**(2), 141–148.

122 M. Li, X. Fu, H. Gao, Y. Ji, J. Li and Y. Wang, Regulation of an osteon-like concentric microgrooved surface on osteogenesis and osteoclastogenesis, *Biomaterials*, 2019, **216**, 119269.

123 A. Pandit, A. Indurkar, J. Locs, H. J. Haugen and D. Loca, Calcium Phosphates: A Key to Next-Generation In Vitro Bone Modeling, *Adv. Healthcare Mater.*, 2024, **13**(29), e2401307.

124 B. Guillotin and F. Guillemot, Cell patterning technologies for organotypic tissue fabrication, *Trends Biotechnol.*, 2011, **29**(4), 183–190.

125 N. E. Fedorovich, W. Schuurman, H. M. Wijnberg, H. J. Prins, P. R. van Weeren and J. Malda, *et al.*, Biofabrication of osteochondral tissue equivalents by printing topologically defined, cell-laden hydrogel scaffolds, *Tissue Eng., Part C*, 2012, **18**(1), 33–44.

126 A. Schwab, C. Helary, R. G. Richards, M. Alini, D. Eglin and M. D'Este, Tissue mimetic hyaluronan bioink containing collagen fibers with controlled orientation modulating cell migration and alignment, *Mater. Today Bio*, 2020, **7**, 100058.

127 T. Ahlfeld, F. P. Schuster, Y. Forster, M. Quade, A. R. Akkineni and C. Rentsch, *et al.*, 3D Plotted Biphasic Bone Scaffolds for Growth Factor Delivery: Biological Characterization In Vitro and In Vivo, *Adv. Healthcare Mater.*, 2019, **8**(7), e1801512.

128 N. Raja, H. Park, Y. J. Choi and H. S. Yun, Multifunctional Calcium-Deficient Hydroxyl Apatite-Alginate Core-Shell-Structured Bone Substitutes as Cell and Drug Delivery Vehicles for Bone Tissue Regeneration, *ACS Biomater. Sci. Eng.*, 2021, **7**(3), 1123–1133.

129 M. F. Kunrath, F. M. Diz, R. Magini and M. E. Galarraga-Vinueza, Nanointeraction: The profound influence of nanostructured and nano-drug delivery biomedical implant surfaces on cell behavior, *Adv. Colloid Interface Sci.*, 2020, **284**, 102265.

130 E. R. Urquia Edreira, A. Hayrapetyan, J. G. Wolke, H. J. Croes, A. Klymov and J. A. Jansen, *et al.*, Effect of calcium phosphate ceramic substrate geometry on mesenchymal stromal cell organization and osteogenic differentiation, *Biofabrication*, 2016, **8**(2), 025006.

131 L. Lv, Y. Liu, P. Zhang, X. Bai, X. Ma and Y. Wang, *et al.*, The epigenetic mechanisms of nanotopography-guided osteogenic differentiation of mesenchymal stem cells via high-throughput transcriptome sequencing, *Int. J. Nanomed.*, 2018, **13**, 5605–5623.

132 N. I. Aminuddin, R. Ahmad, S. A. Akbar and B. Pingguan-Murphy, Osteoblast and stem cell response to nanoscale topographies: a review, *Sci. Technol. Adv. Mater.*, 2016, **17**(1), 698–714.



133 J. Chi, M. Wang, J. Chen, L. Hu, Z. Chen and L. J. Backman, *et al.*, Topographic Orientation of Scaffolds for Tissue Regeneration: Recent Advances in Biomaterial Design and Applications, *Biomimetics*, 2022, **7**(3), 131.

134 Q. Wang, Y. Huang and Z. Qian, Nanostructured Surface Modification to Bone Implants for Bone Regeneration, *J. Biomed. Nanotechnol.*, 2018, **14**(4), 628–648.

135 M. A. Fernandez-Yague, S. A. Abbah, L. McNamara, D. I. Zeugolis, A. Pandit and M. J. Biggs, Biomimetic approaches in bone tissue engineering: Integrating biological and physicomechanical strategies, *Adv. Drug Delivery Rev.*, 2015, **84**, 1–29.

136 A. J. Engler, S. Sen, H. L. Sweeney and D. E. Discher, Matrix elasticity directs stem cell lineage specification, *Cell*, 2006, **126**(4), 677–689.

137 Z. Li, Y. Gong, S. Sun, Y. Du, D. Lu and X. Liu, *et al.*, Differential regulation of stiffness, topography, and dimension of substrates in rat mesenchymal stem cells, *Biomaterials*, 2013, **34**(31), 7616–7625.

138 M. J. Mirzaali, J. J. Schwiedrzik, S. Thaivichai, J. P. Best, J. Michler and P. K. Zysset, *et al.*, Mechanical properties of cortical bone and their relationships with age, gender, composition and microindentation properties in the elderly, *Bone*, 2016, **93**, 196–211.

139 D. Wu, P. Isaksson, S. J. Ferguson and C. Persson, Young's modulus of trabecular bone at the tissue level: A review, *Acta Biomater.*, 2018, **78**, 1–12.

140 N. Huebsch, P. R. Arany, A. S. Mao, D. Shvartsman, O. A. Ali and S. A. Bencherif, *et al.*, Harnessing traction-mediated manipulation of the cell/matrix interface to control stem-cell fate, *Nat. Mater.*, 2010, **9**(6), 518–526.

141 R. Olivares-Navarrete, E. M. Lee, K. Smith, S. L. Hyzy, M. Doroudi and J. K. Williams, *et al.*, Substrate Stiffness Controls Osteoblastic and Chondrocytic Differentiation of Mesenchymal Stem Cells without Exogenous Stimuli, *PLoS One*, 2017, **12**(1), e0170312.

142 J. Zhang, E. Wehrle, P. Adamek, G. R. Paul, X. H. Qin and M. Rubert, *et al.*, Optimization of mechanical stiffness and cell density of 3D bioprinted cell-laden scaffolds improves extracellular matrix mineralization and cellular organization for bone tissue engineering, *Acta Biomater.*, 2020, **114**, 307–322.

143 G. Chen, C. Dong, L. Yang and Y. Lv, 3D Scaffolds with Different Stiffness but the Same Microstructure for Bone Tissue Engineering, *ACS Appl. Mater. Interfaces*, 2015, **7**(29), 15790–15802.

144 E. Neto, A. C. Monteiro, C. Leite Pereira, M. Simoes, J. P. Conde and V. Chu, *et al.*, Micropathological Chip Modeling the Neurovascular Unit Response to Inflammatory Bone Condition, *Adv. Healthcare Mater.*, 2022, **11**(11), e2102305.

145 C. Ming Leung, P. de Haan, G. Kim, J. Ko and H. S. Rho, *et al.*, A guide to the organ-on-a-chip, *Nat. Rev. Methods Primers*, 2022, **2**(1), 33.

146 J. H. Sung, M. B. Esch, J. M. Prot, C. J. Long, A. Smith and J. J. Hickman, *et al.*, Microfabricated mammalian organ systems and their integration into models of whole animals and humans, *Lab Chip*, 2013, **13**(7), 1201–1212.

147 E. W. Esch, A. Bahinski and D. Huh, Organs-on-chips at the frontiers of drug discovery, *Nat. Rev. Drug Discovery*, 2015, **14**(4), 248–260.

148 N. Picollet-D'hahan, A. Zuchowska, I. Lemeunier and S. Le Gac, Multiorgan-on-a-Chip: A Systemic Approach To Model and Decipher Inter-Organ Communication, *Trends Biotechnol.*, 2021, **39**(8), 788–810.

149 R. Barrile, A. D. van der Meer, H. Park, J. P. Fraser, D. Simic and F. Teng, *et al.*, Organ-on-Chip Recapitulates Thrombosis Induced by an anti-CD154 Monoclonal Antibody: Translational Potential of Advanced Microengineered Systems, *Clin. Pharmacol. Ther.*, 2018, **104**(6), 1240–1248.

150 C. Yvanoff and R. G. Willaert, Development of bone cell microarrays in microfluidic chips for studying osteocyte-osteoblast communication under fluid flow mechanical loading, *Biofabrication*, 2022, **14**(2), 025014.

151 J. H. Lee, Y. Gu, H. Wang and W. Y. Lee, Microfluidic 3D bone tissue model for high-throughput evaluation of wound-healing and infection-preventing biomaterials, *Biomaterials*, 2012, **33**(4), 999–1006.

152 S. H. Park, W. Y. Sim, B. H. Min, S. S. Yang, A. Khademhosseini and D. L. Kaplan, Chip-based comparison of the osteogenesis of human bone marrow- and adipose tissue-derived mesenchymal stem cells under mechanical stimulation, *PLoS One*, 2012, **7**(9), e46689.

153 Y. S. Torisawa, C. S. Spina, T. Mammoto, A. Mammoto, J. C. Weaver and T. Tat, *et al.*, Bone marrow-on-a-chip replicates hematopoietic niche physiology in vitro, *Nat. Methods*, 2014, **11**(6), 663–669.

154 N. Jusoh, S. Oh, S. Kim, J. Kim and N. L. Jeon, Microfluidic vascularized bone tissue model with hydroxyapatite-incorporated extracellular matrix, *Lab Chip*, 2015, **15**(20), 3984–3988.

155 S. Bersini, M. Gilardi, C. Arrigoni, G. Talo, M. Zamai and L. Zagra, *et al.*, Human in vitro 3D co-culture model to engineer vascularized bone-mimicking tissues combining computational tools and statistical experimental approach, *Biomaterials*, 2016, **76**, 157–172.

156 S. Sieber, L. Wirth, N. Cavak, M. Koenigsmark, U. Marx and R. Lauster, *et al.*, Bone marrow-on-a-chip: Long-term culture of human haematopoietic stem cells in a three-dimensional microfluidic environment, *J. Tissue Eng. Regener. Med.*, 2018, **12**(2), 479–489.

157 K. Middleton, S. Al-Dujaili, X. Mei, A. Gunther and L. You, Microfluidic co-culture platform for investigating osteocyte-osteoclast signalling during fluid shear stress mechanostimulation, *J. Biomech.*, 2017, **59**, 35–42.

158 Q. Sun, S. Choudhary, C. Mannion, Y. Kissin, J. Zilberman and W. Y. Lee, Ex vivo replication of phenotypic functions of osteocytes through biomimetic 3D bone tissue construction, *Bone*, 2018, **106**, 148–155.

159 H. P. Ma, X. Deng, D. Y. Chen, D. Zhu, J. L. Tong and T. Zhao, *et al.*, A microfluidic chip-based co-culture of fibroblast-like synoviocytes with osteoblasts and osteoclasts to test bone erosion and drug evaluation, *R. Soc. Open Sci.*, 2018, **5**(9), 180528.



160 N. Movilla, C. Borau, C. Valero and J. M. Garcia-Aznar, Degradation of extracellular matrix regulates osteoblast migration: A microfluidic-based study, *Bone*, 2018, **107**, 10–17.

161 E. Babaliari, G. Petekidis and M. Chatzinkolaidou, A Precisely Flow-Controlled Microfluidic System for Enhanced Pre-Osteoblastic Cell Response for Bone Tissue Engineering, *Bioengineering*, 2018, **5**(3), 66.

162 S. S. Kotha, B. J. Hayes, K. T. Phong, M. A. Redd, K. Bomsztyk and A. Ramakrishnan, *et al.*, Engineering a multicellular vascular niche to model hematopoietic cell trafficking, *Stem Cell Res. Ther.*, 2018, **9**(1), 77.

163 S. L. Truesdell, E. L. George, C. C. Van Vranken and M. M. Saunders, A Lab-On-A-Chip Platform for Stimulating Osteocyte Mechanotransduction and Analyzing Functional Outcomes of Bone Remodeling, *J. Visualized Exp.*, 2020(159), e61076.

164 P. Alaman-Diez, E. Garcia-Gareta, M. Arruebo and M. A. Perez, A bone-on-a-chip collagen hydrogel-based model using pre-differentiated adipose-derived stem cells for personalized bone tissue engineering, *J. Biomed. Mater. Res., Part A*, 2023, **111**(1), 88–105.

165 L. Xu, X. Song, G. Carroll and L. You, Novel in vitro microfluidic platform for osteocyte mechanotransduction studies, *Integr. Biol.*, 2020, **12**(12), 303–310.

166 E. L. George, S. L. Truesdell, S. L. York and M. M. Saunders, Lab-on-a-chip platforms for quantification of multicellular interactions in bone remodeling, *Exp. Cell Res.*, 2018, **365**(1), 106–118.

167 V. P. Z. A. Galván-Chacón, B. Hesse, M. Bohner, P. Habibovic and D. Barata, Bone-on-a-Chip: A Microscale 3D Biomimetic Model to Study Bone Regeneration, *Adv. Eng. Mater.*, 2022, **24**(7), 13.

168 J. W. Park, B. Vahidi, A. M. Taylor, S. W. Rhee and N. L. Jeon, Microfluidic culture platform for neuroscience research, *Nat. Protoc.*, 2006, **1**(4), 2128–2136.

169 D. I. Silva, B. P. D. Santos, J. Leng, H. Oliveira and J. Amedee, Dorsal root ganglion neurons regulate the transcriptional and translational programs of osteoblast differentiation in a microfluidic platform, *Cell Death Dis.*, 2017, **8**(12), 3209.

170 C. Pak, N. S. Callander, E. W. Young, B. Titz, K. Kim and S. Saha, *et al.*, MicroC(3), an ex vivo microfluidic cis-coculture assay to test chemosensitivity and resistance of patient multiple myeloma cells, *Integr. Biol.*, 2015, **7**(6), 643–654.

171 S. M. Bonk, M. Stubbe, S. M. Buehler, C. Tautorat, W. Baumann and E. D. Klinkenberg, *et al.*, Design and Characterization of a Sensorized Microfluidic Cell-Culture System with Electro-Thermal Micro-Pumps and Sensors for Cell Adhesion, Oxygen, and pH on a Glass Chip, *Biosensors*, 2015, **5**(3), 513–536.

172 M. V. Lipreri, G. Di Pompeo, E. Boanini, G. Graziani, E. Sassoni and N. Baldini, *et al.*, Bone on-a-chip: a 3D dendritic network in a screening platform for osteocyte-targeted drugs, *Biofabrication*, 2023, **15**(4), 045019.

173 K. Paek, S. Kim, S. Tak, M. K. Kim, J. Park and S. Chung, *et al.*, A high-throughput biomimetic bone-on-a-chip platform with artificial intelligence-assisted image analysis for osteoporosis drug testing, *Bioeng. Transl. Med.*, 2023, **8**(1), e10313.

174 A. Marturano-Kruik, M. M. Nava, K. Yeager, A. Chramiec, L. Hao and S. Robinson, *et al.*, Human bone perivascular niche-on-a-chip for studying metastatic colonization, *Proc. Natl. Acad. Sci. U. S. A.*, 2018, **115**(6), 1256–1261.

175 M. Orciani, M. Fini, R. Di Primio and M. Mattioli-Belmonte, Biofabrication and Bone Tissue Regeneration: Cell Source, Approaches, and Challenges, *Front. Bioeng. Biotechnol.*, 2017, **5**, 17.

176 J. Ahn, Y. J. Sei, N. L. Jeon and Y. Kim, Tumor Microenvironment on a Chip: The Progress and Future Perspective, *Bioengineering*, 2017, **4**(3), 64.

177 Y. Pan, N. Hu, X. Wei, L. Gong, B. Zhang and H. Wan, *et al.*, 3D cell-based biosensor for cell viability and drug assessment by 3D electric cell/matrix-substrate impedance sensing, *Biosens. Bioelectron.*, 2019, **130**, 344–351.

178 S. Fuchs, S. Johansson, A. O. Tjell, G. Werr, T. Mayr and M. Tenje, In-Line Analysis of Organ-on-Chip Systems with Sensors: Integration, Fabrication, Challenges, and Potential, *ACS Biomater. Sci. Eng.*, 2021, **7**(7), 2926–2948.

179 G. David Roodman and R. Silbermann, Mechanisms of osteolytic and osteoblastic skeletal lesions, *BoneKEy Rep.*, 2015, **4**, 753.

180 J. S. Jeon, S. Bersini, M. Gilardi, G. Dubini, J. L. Charest and M. Moretti, *et al.*, Human 3D vascularized organotypic microfluidic assays to study breast cancer cell extravasation, *Proc. Natl. Acad. Sci. U. S. A.*, 2015, **112**(1), 214–219.

181 M. Houshmand, M. Soleimani, A. Atashi, G. Saglio, M. Abdollahi and M. Nikougoftar Zarif, Mimicking the Acute Myeloid Leukemia Niche for Molecular Study and Drug Screening, *Tissue Eng., Part C*, 2017, **23**(2), 72–85.

182 S. Hao, L. Ha, G. Cheng, Y. Wan, Y. Xia and D. M. Sosnoski, *et al.*, A Spontaneous 3D Bone-On-a-Chip for Bone Metastasis Study of Breast Cancer Cells, *Small*, 2018, **14**(12), e1702787.

183 X. Mei, K. Middleton, D. Shim, Q. Wan, L. Xu and Y. V. Ma, *et al.*, Microfluidic platform for studying osteocyte mechanoregulation of breast cancer bone metastasis, *Integr. Biol.*, 2019, **11**(4), 119–129.

184 J. Ahn, J. Lim, N. Jusoh, J. Lee, T. E. Park and Y. Kim, *et al.*, 3D Microfluidic Bone Tumor Microenvironment Comprised of Hydroxyapatite/Fibrin Composite, *Front. Bioeng. Biotechnol.*, 2019, **7**, 168.

185 S. W. Verbruggen, C. L. Thompson, M. P. Duffy, S. Lunetto, J. Nolan and O. M. T. Pearce, *et al.*, Mechanical Stimulation Modulates Osteocyte Regulation of Cancer Cell Phenotype, *Cancers*, 2021, **13**(12), 2906.

186 S. Bersini, J. S. Jeon, G. Dubini, C. Arrigoni, S. Chung and J. L. Charest, *et al.*, A microfluidic 3D in vitro model for specificity of breast cancer metastasis to bone, *Biomaterials*, 2014, **35**(8), 2454–2461.



187 J. Kong, Y. Luo, D. Jin, F. An, W. Zhang and L. Liu, *et al.*, A novel microfluidic model can mimic organ-specific metastasis of circulating tumor cells, *Onco Targets Ther.*, 2016, **7**(48), 78421–78432.

188 P. Ziegler, A. D. Hartkopf, M. Wallwiener, L. Haberle, H. C. Kolberg and P. Hadji, *et al.*, The impact of physical activity on progression-free and overall survival in metastatic breast cancer based on molecular subtype, *BMC Cancer*, 2024, **24**(1), 1284.

189 E. A. Margolis, D. S. Cleveland, Y. P. Kong, J. A. Beamish, W. Y. Wang and B. M. Baker, *et al.*, Stromal cell identity modulates vascular morphogenesis in a microvasculature-on-a-chip platform, *Lab Chip*, 2021, **21**(6), 1150–1163.

190 L. E. Bertassoni, M. Ceconi, V. Manoharan, M. Nikkhah, J. Hjortnaes and A. L. Cristina, *et al.*, Hydrogel bioprinted microchannel networks for vascularization of tissue engineering constructs, *Lab Chip*, 2014, **14**(13), 2202–2211.

191 C. J. Alves, I. S. Alencastre, E. Neto, J. Ribas, S. Ferreira and D. M. Vasconcelos, *et al.*, Bone Injury and Repair Trigger Central and Peripheral NPY Neuronal Pathways, *PLoS One*, 2016, **11**(11), e0165465.

192 D. Song, X. Jiang, S. Zhu, W. Li, A. Khadka and J. Hu, Denervation impairs bone regeneration during distraction osteogenesis in rabbit tibia lengthening, *Acta Orthop.*, 2012, **83**(4), 406–410.

193 G. Thrivikraman, A. Athirasala, R. Gordon, L. Zhang, R. Bergan and D. R. Keene, *et al.*, Rapid fabrication of vascularized and innervated cell-laden bone models with biomimetic intrafibrillar collagen mineralization, *Nat. Commun.*, 2019, **10**(1), 3520.

194 D. Pamies, A. Bal-Price, C. Chesne, S. Coecke, A. Dinnyes and C. Eskes, *et al.*, Advanced Good Cell Culture Practice for human primary, stem cell-derived and organoid models as well as microphysiological systems, *ALTEX*, 2018, **35**(3), 353–378.

195 P. Jennings, The future of in vitro toxicology, *Toxicol. In Vitro*, 2015, **29**(6), 1217–1221.

196 G. Stacey, Current developments in cell culture technology, *Adv. Exp. Med. Biol.*, 2012, **745**, 1–13.

197 C. Patel, L. Shi, J. F. Whitesides, B. M. Foster, R. J. Fajardo and E. E. Quillen, *et al.*, A New Method of Bone Stromal Cell Characterization by Flow Cytometry, *Curr. Protoc.*, 2022, **2**(3), e400.

198 H. Akagi, Y. Tanaka, K. Wada, M. Takahashi, K. Yoshida and H. Domoto, CDX2-positive Cancer of Unknown Primary With Upper-body Paralysis Was Dramatically Improved by Colorectal Cancer Chemotherapy, *Anticancer Res.*, 2023, **43**(6), 2879–2884.

199 A. Roth and T. Singer, The application of 3D cell models to support drug safety assessment: opportunities & challenges, *Adv. Drug Delivery Rev.*, 2014, **69**–**70**, 179–189.

200 I. Maschmeyer, T. Hasenberg, A. Jaenicke, M. Lindner, A. K. Lorenz and J. Zech, *et al.*, Chip-based human liver-intestine and liver-skin co-cultures—A first step toward systemic repeated dose substance testing in vitro, *Eur. J. Pharm. Biopharm.*, 2015, **95**(Pt A), 77–87.

201 W. Zhang, W. Y. Lee, D. S. Siegel, P. Tolias and J. Zilberberg, Patient-specific 3D microfluidic tissue model for multiple myeloma, *Tissue Eng., Part C*, 2014, **20**(8), 663–670.

202 P. Neri and N. J. Bahlis, Targeting of adhesion molecules as a therapeutic strategy in multiple myeloma, *Curr. Cancer Drug Targets*, 2012, **12**(7), 776–796.

203 Z. P. Khin, M. L. Ribeiro, T. Jacobson, L. Hazlehurst, L. Perez and R. Baz, *et al.*, A preclinical assay for chemosensitivity in multiple myeloma, *Cancer Res.*, 2014, **74**(1), 56–67.

204 W. Xiao, L. Xin, R. Cao, X. Wu, R. Tian and L. Che, *et al.*, Sensing morphogenesis of bone cells under microfluidic shear stress by holographic microscopy and automatic aberration compensation with deep learning, *Lab Chip*, 2021, **21**(7), 1385–1394.

205 D. Zuncheddu, E. Della Bella, A. Schwab, D. Petta, G. Rocchitta and S. Generelli, *et al.*, Quality control methods in musculoskeletal tissue engineering: from imaging to biosensors, *Bone Res.*, 2021, **9**(1), 46.

206 J. Leighton, R. Mark and G. Justh, Patterns of three-dimensional growth in vitro in collagen-coated cellulose sponge: carcinomas and embryonic tissues, *Cancer Res.*, 1968, **28**(2), 286–296.

